

*Supporting Information
for*

**Effects of π -Conjugation on the Solid-State Photoresponsive Coloring Behavior of
Bipyridine-Boronium Complexes**

Junro Yoshino,^{**a,b*} Yoshito Hirono,^{*b*} Ryota Akahane,^{*b*} Hiroyuki Higuchi,^{*b*} and Naoto Hayashi^{*a,b*}

^{*a*} Faculty of Science, University of Toyama, 3190 Gofuku, Toyama, Toyama 930-8555, Japan.

^{*b*} Department of Chemistry, Graduate School of Science and Engineering, University of Toyama, 3190 Gofuku, Toyama, Toyama 930-8555, Japan.

E-mail: yoshino@sci.u-toyama.ac.jp

Contents

1. Tables and Figures	page S3
Table S1	Longest-wavelength absorption maxima, molar absorption coefficients, absorption-onset wavelengths, fluorescence maxima, and fluorescence quantum yields of 1 , 2a–e , and 3a–d in MeCN
Table S2	Photographs showing colors of solids before and after UV irradiation, and newly appeared absorption maxima after UV irradiation
Table S3	Color-quenching rate constants of photoirradiated PMMA films containing compound 1 and 2a–d
Figure S1–S5	ORTEP drawings of 2a ·CHCl ₃ , 2b ·CHCl ₃ , 2c ·2CHCl ₃ , 3a , and 3d
Figure S6	Calculated energy levels of frontier molecular orbitals of 1' , 2a'-e' , and 3a'-d'
Figure S7	Calculated singlet excitation energy levels of 1' , 2a'-e' , and 3a'-d'
Figure S8–S16	UV-vis absorption and fluorescence spectra in MeCN, and diffuse reflection spectra of 2a–e and 3a–d in the solid state
Figure S17–S21	Absorption spectra of PMMA films containing compound 2a–e before and after UV irradiation
Figure S22	Diffuse reflection spectra of compound 3a in the solid state before and after UV irradiation
Figure S23	Absorption spectra of a PMMA film containing compound 1 before and after UV irradiation
Figure S24–S26	Packing structures of 2a ·CHCl ₃ , 2b ·CHCl ₃ , and 2c ·2CHCl ₃

Figure S27–S30	X-ray powder diffraction patterns of 1 and 2a–c
Scheme S1	Two phases of the process after irradiation of the boronium complex
Scheme S2	A hypothetical reaction and coloring product in Scheme S1
2. Experimental section	page S25
General information	
Synthesis	
Polymer film experiments	
X-ray crystallographic analysis	
X-ray powder diffraction	
Theoretical calculations	
3. NMR spectra	page S48
4. References	page S59

1. Tables and Figures

Table S1. Longest-wavelength absorption maxima (λ_{abs}), molar absorption coefficients (ε), absorption-onset wavelengths (λ_{onset}), fluorescence maxima (λ_{fl}), and fluorescence quantum yields (Φ_{F}) of **1**, **2a–e**, and **3a–d** in MeCN.

Compound	$\lambda_{\text{abs}}/\text{nm}$ ($\varepsilon/\text{M}^{-1}\text{cm}^{-1}$)	$\lambda_{\text{onset}}^b/\text{nm}$	$\lambda_{\text{fl}}/\text{nm}$	Φ_{F}
2a	327 (3.1×10^4), [347 (1.2×10^4)] ^a	407	504	0.50
2b	355 (3.8×10^4)	414	503	0.16
2c	356 (4.0×10^4)	415	505	0.24
2d	347 (4.6×10^4)	411	516	0.34
2e	317 (2.0×10^4), [340 (9.3×10^3)] ^a	395	496	0.42
3a	356 (3.5×10^4)	390	425	0.28
3b	397 (3.2×10^4)	442	476	0.60
3c	418 (1.7×10^4)	451	488	0.98
3d	386 (5.0×10^4)	426	478	0.39
1^[1]	315 (1.3×10^4), [335 (2.9×10^3)] ^a	395	495	0.21

^a Shoulder. ^b λ_{onset} was determined as the wavelength corresponding to the intersection of the base line and a straight line joining two points on the spectrum with half and quarter the intensities relative to that of the longest-wavelength absorption maxima or shoulder.

Table S2. Photographs showing colors of solids before and after UV irradiation, and newly appeared absorption maxima (λ) after UV irradiation

Compounds	Before irradiation	After irradiation	λ/nm
2a		 pink ^a	
		 (in film, during UV irradiation)	556 ^d
		 (in film)	
2b		 pink ^a	572 ^d
2c		 orange ^a	570 ^d
2d		 orange ^a	559 ^d
2e		 pink ^a	546 ^d
3a		 pale orange ^b	
		 orange ^a	566 ^e
3b		— ^c	— ^f
3c		— ^c	— ^f
3d		— ^c	— ^f
1	colorless ¹	red orange ^{b,1}	527 ^{e,1} , 529 ^d

^a Under nitrogen atmosphere. ^b In air. ^c No color change upon UV irradiation even under nitrogen atmosphere. ^d Observed in absorption spectra of the PMMA film. ^e Observed in diffuse reflection spectra of the powder solid. ^f No data.

Table S3. Color-quenching rate constants k of the photoirradiated PMMA films containing dispersed compound **1** and **2a–d**^a

Compound	$10^{-3} k / \text{s}^{-1}$ ^b	Observation wavelength/nm
1	3.7 (0.3)	530
2a	4.27 (0.19)	555
2b	2.81 (0.06)	573
2c	1.70 (0.12)	570
2d	4.2 (0.5)	560

^a Although the oxygen concentration in the PMMA film was low, the estimated amount of photogenerated colored species in the film was also quite small. Estimation of color-quenching rate constants was carried out under the assumption that the reaction of the photogenerated colored species with oxygen was a pseudo first-order reaction.

^b Values in parentheses are standard errors.

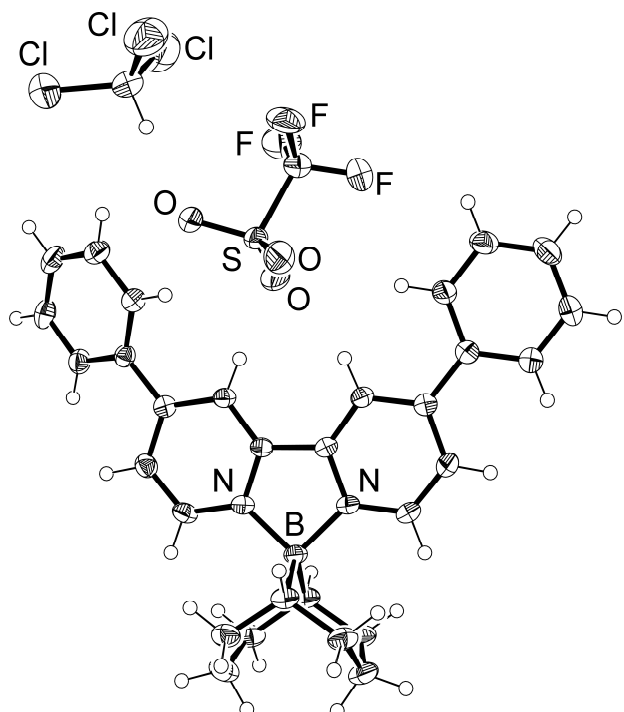


Figure S1. ORTEP drawing of **2a**·CHCl₃ (50% probability). Selected bond lengths: B–N = 1.611(3) and 1.615(3) Å; B–C = 1.610(3) and 1.615(2) Å. Selected bond angles: N–B–N = 94.60(13)°; C–B–C = 107.22(15)°; N–B–C = 116.24(15)°, 111.49(15)°, 114.56(15)°, and 112.53(15)°. Selected dihedral angles: pyridine ring–benzene ring = 26.1(2)° and 0.8(2)°.

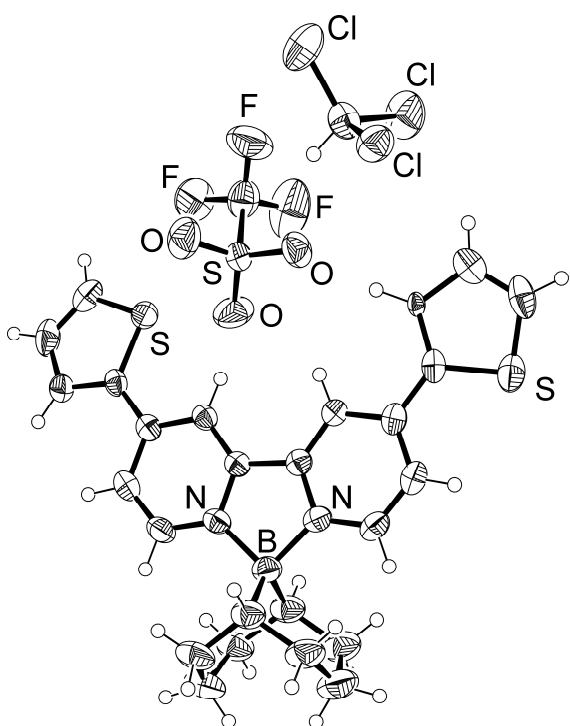


Figure S2. ORTEP drawing of **2b**·CHCl₃ (50% probability). One of the two crystallographically independent species set is shown. Selected bond lengths: B–N = 1.608(5) and 1.620(6) Å [1.606(6) and 1.620(6) Å]; B–C = 1.612(5) and 1.618(6) Å [1.594(6) and 1.612(6) Å]. Selected bond angles: N–B–N = 95.0(3)° [94.6(3)°]; C–B–C = 106.8(3)° [107.6(3)°]; N–B–C = 113.1(3)°, 113.5(3)°, 116.3(3)°, and 112.2(3)° [115.2(3)°, 112.5(3)°, 115.8(4)°, and 111.0(3)°]. Selected dihedral angles: pyridine ring–thiophene ring = 4.0(5)° and 14.7(5)° [3.1(5)° and 13.8(5)°].

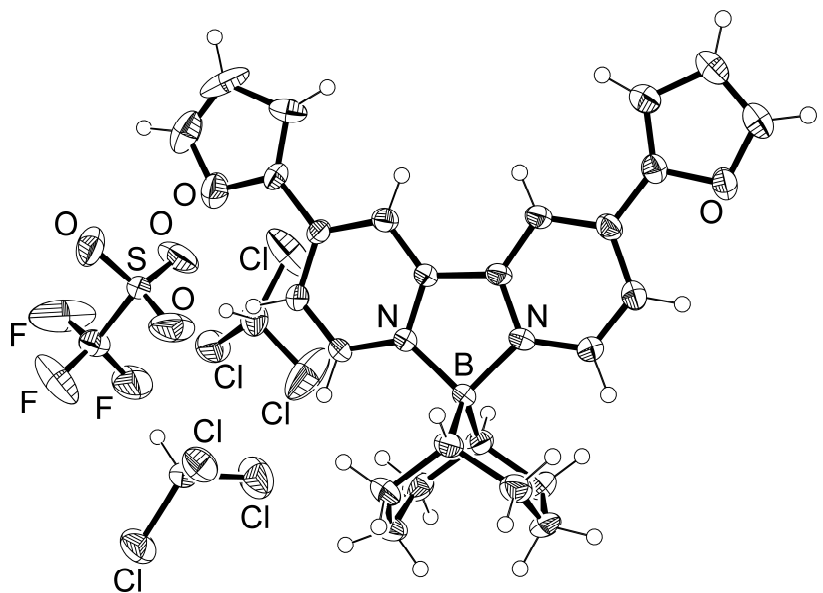


Figure S3. ORTEP drawing of **2c**·2CHCl₃ (50% probability). Selected bond lengths: B–N = 1.597(6) and 1.608(6) Å; B–C = 1.618(7) and 1.616(7) Å. Selected bond angles: N–B–N = 94.4(3)°; C–B–C = 107.7(4)°; N–B–C = 112.8(4)°, 114.5(4)°, 112.9(4)°, and 114.2(4)°. Selected dihedral angles: pyridine ring–furan ring = 1.4(7)° and 2.6(7)°.

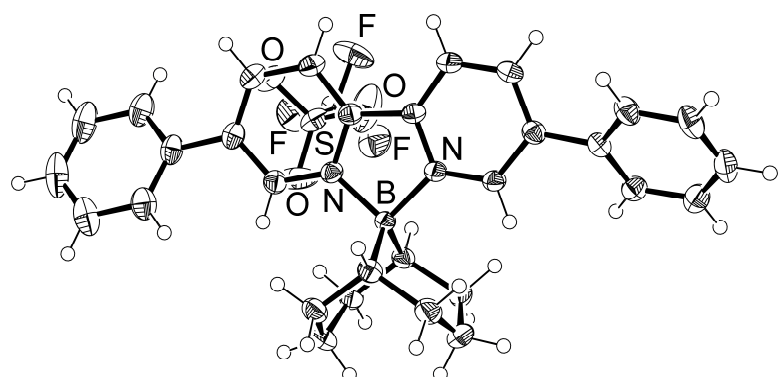


Figure S4. ORTEP drawing of **3a** (50% probability). Selected bond lengths: B–N = 1.612(2) and 1.606(2) Å; B–C = 1.615(2) and 1.6139(19) Å. Selected bond angles: N–B–N = 95.01(10)°; C–B–C = 107.74(11)°; N–B–C = 113.50(12)°, 113.90(14)°, 112.91(14)°, and 113.58(11)°. Selected dihedral angles: pyridine ring–benzene ring = 31.2(2)° and 41.2(2)°.

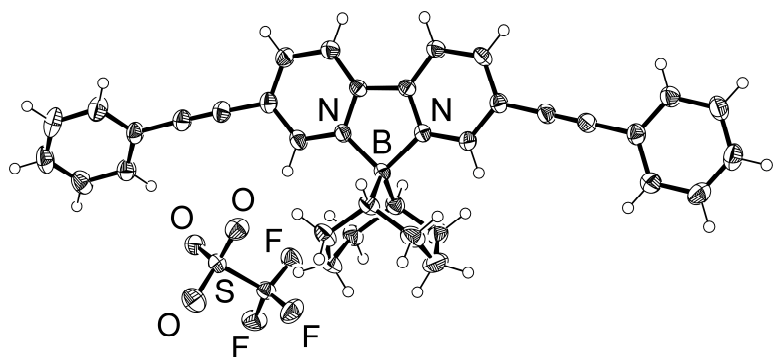


Figure S5. ORTEP drawing of **3d** (50% probability). Selected bond lengths: B–N = 1.617(2) and 1.607(2) Å; B–C = 1.611(3) and 1.605(2) Å. Selected bond angles: N–B–N = 95.00(13)°; C–B–C = 107.67(16)°; N–B–C = 114.00(14)°, 112.45(10)°, 113.88(11)°, and 113.65(14)°. Dihedral angles: pyridine ring–benzene ring = 40.7° and 1.9°.

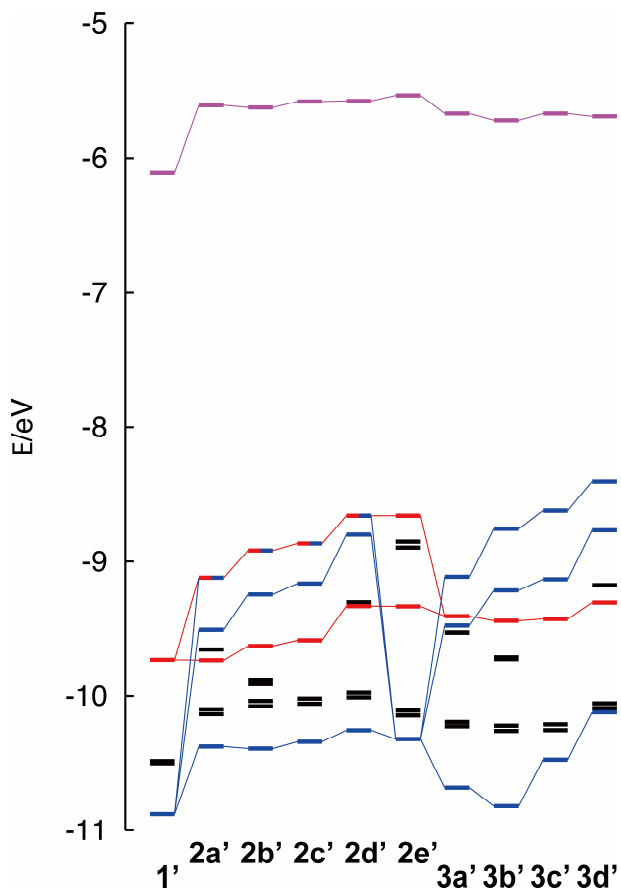


Figure S6. Energy levels of frontier molecular orbitals of **1'**, **2a'-e'**, and **3a'-d'** calculated at the B3LYP/6-31G(d) level of theory. The levels in purple are LUMOs, which are attributed to the π^* orbitals of bpy moieties. All other levels correspond to occupied orbitals. Energy levels in red are concentrated on BBN moieties, consist of B–C σ bonds. Energy levels in blue are the π orbitals of bpy moieties.

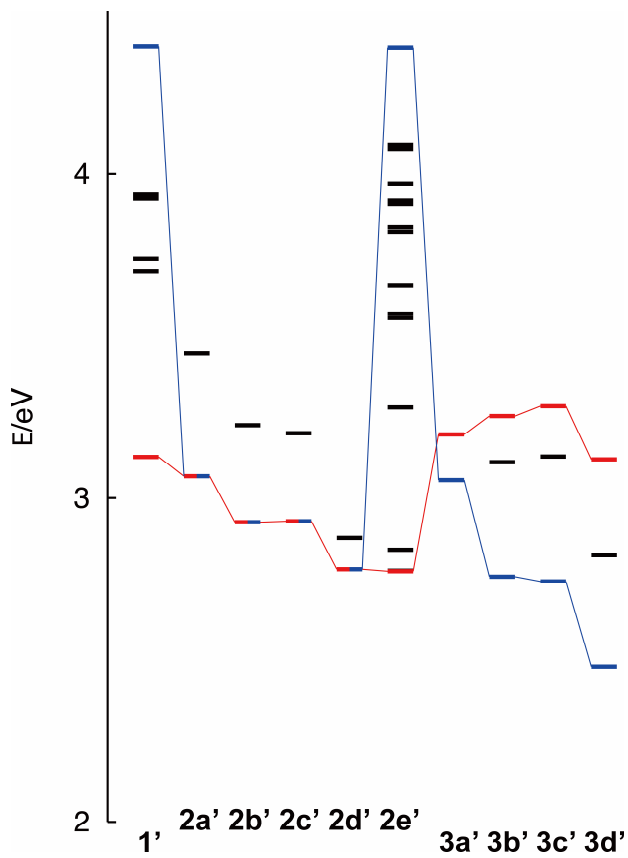


Figure S7. Singlet excitation energy levels of **1'**, **2a'-e'**, and **3a'-d'** calculated at the B3LYP/6-31G(d) level of theory. For each structure, the bottom level corresponds to the lowest singlet excited state (S_1). Red lines denote the lowest-energy states among those corresponding to charge transfer excited electronic configuration from an orbital of the BBN moiety to the bpy π^* orbital. Blue lines denote the lowest-energy states among those corresponding to the $\pi-\pi^*$ ligand-localized excited electronic configuration.

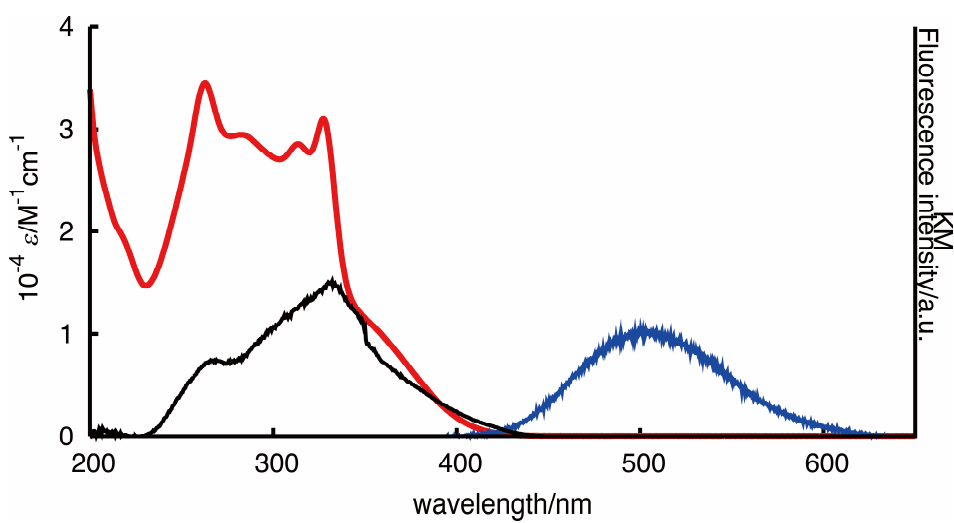


Figure S8. UV-vis absorption (red line) and fluorescence (blue line) spectra of **2a** in MeCN and diffuse reflection spectrum (black line) of **2a** in the solid state.

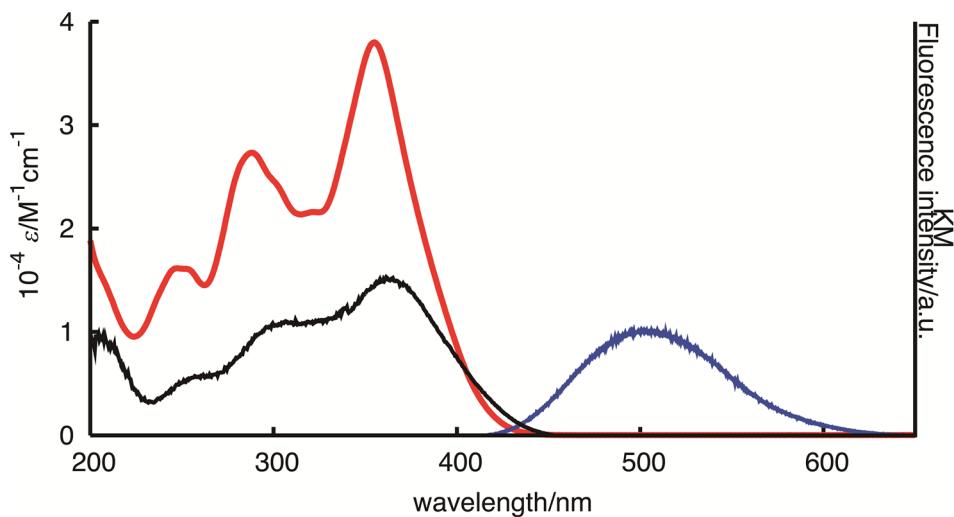


Figure S9. UV-vis absorption (red line) and fluorescence (blue line) spectra of **2b** in MeCN and diffuse reflection spectrum (black line) of **2b** in the solid state.

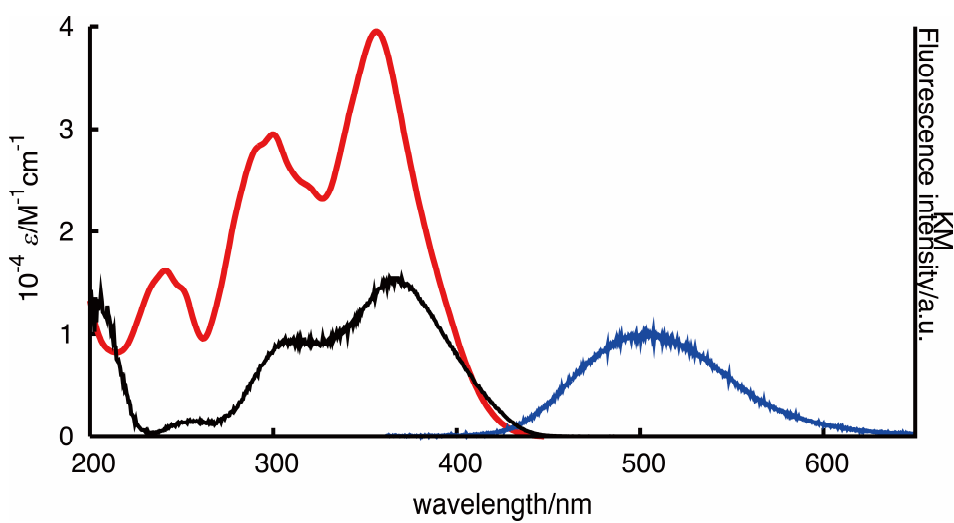


Figure S10. UV-vis absorption (red line) and fluorescence (blue line) spectra of **2c** in MeCN and diffuse reflection spectrum (black line) of **2c** in the solid state.

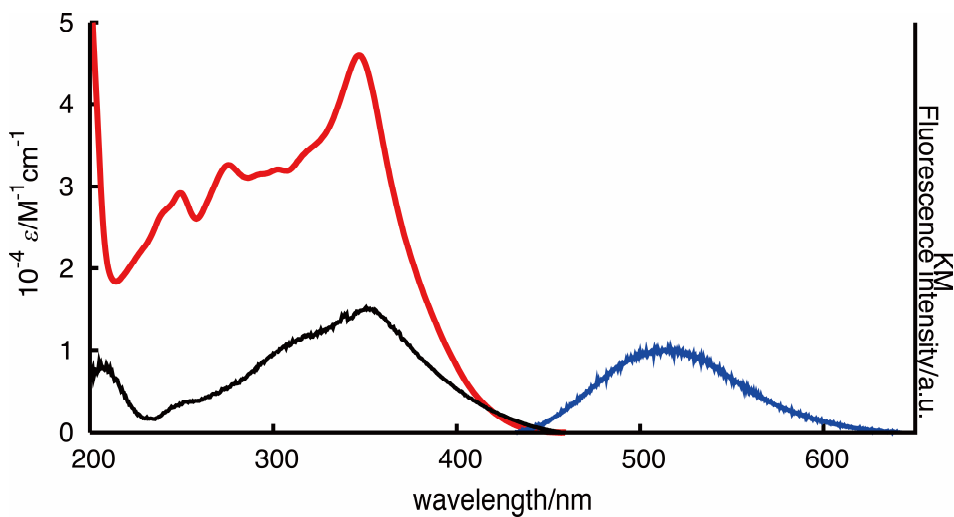


Figure S11. UV-vis absorption (red line) and fluorescence (blue line) spectra of **2d** in MeCN and diffuse reflection spectrum (black line) of **2d** in the solid state.

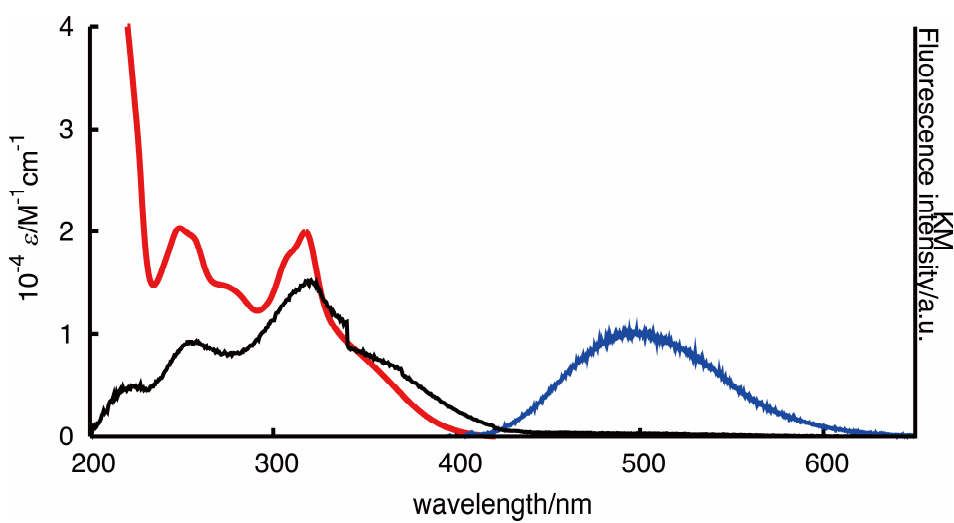


Figure S12. UV-vis absorption (red line) and fluorescence (blue line) spectra of **2e** in MeCN and diffuse reflection spectrum (black line) of **2e** in the solid state.

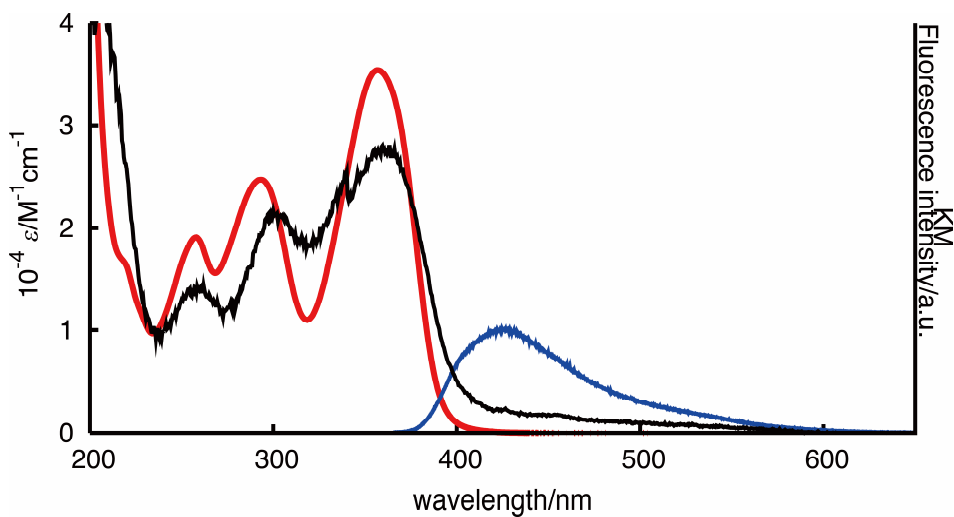


Figure S13. UV-vis absorption (red line) and fluorescence (blue line) spectra of **3a** in MeCN and diffuse reflection spectrum (black line) of **3a** in the solid state.

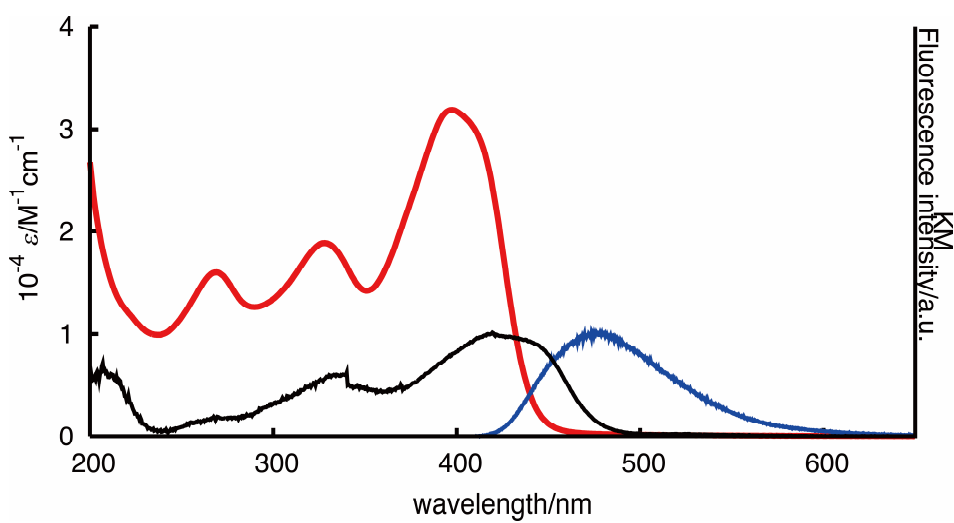


Figure S14. UV-vis absorption (red line) and fluorescence (blue line) spectra of **3b** in MeCN and diffuse reflection spectrum (black line) of **3b** in the solid state.

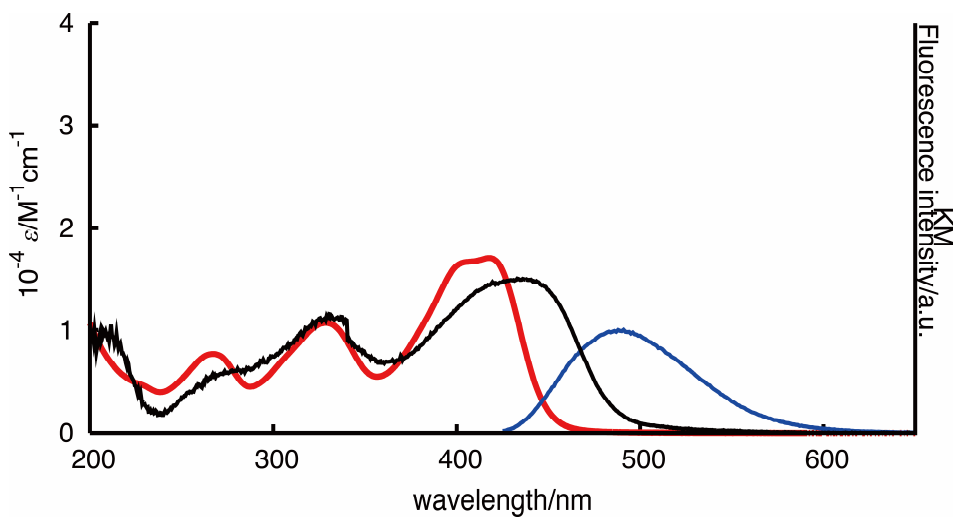


Figure S15. UV-vis absorption (red line) and fluorescence (blue line) spectra of **3c** in MeCN and diffuse reflection spectrum (black line) of **3c** in the solid state.

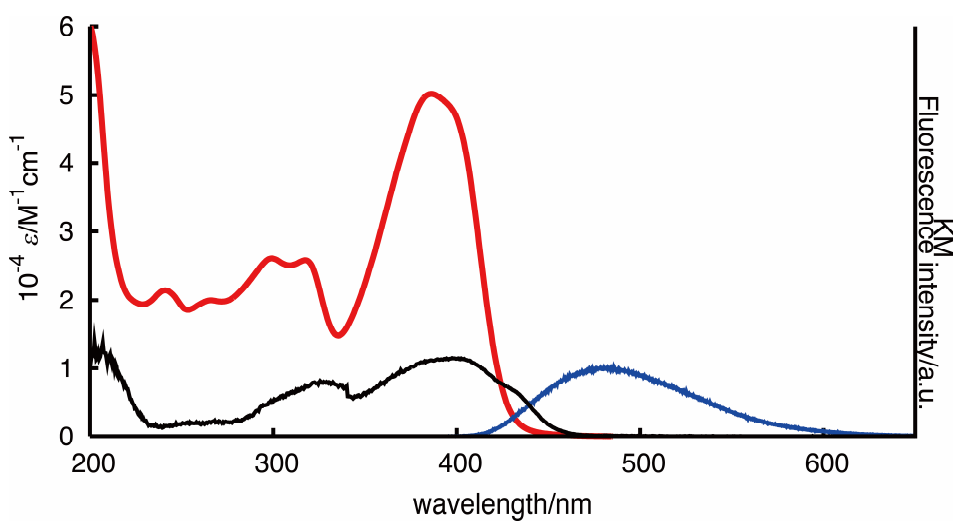


Figure S16. UV-vis absorption (red line) and fluorescence (blue line) spectra of **3d** in MeCN and diffuse reflection spectrum (black line) of **3d** in the solid state.

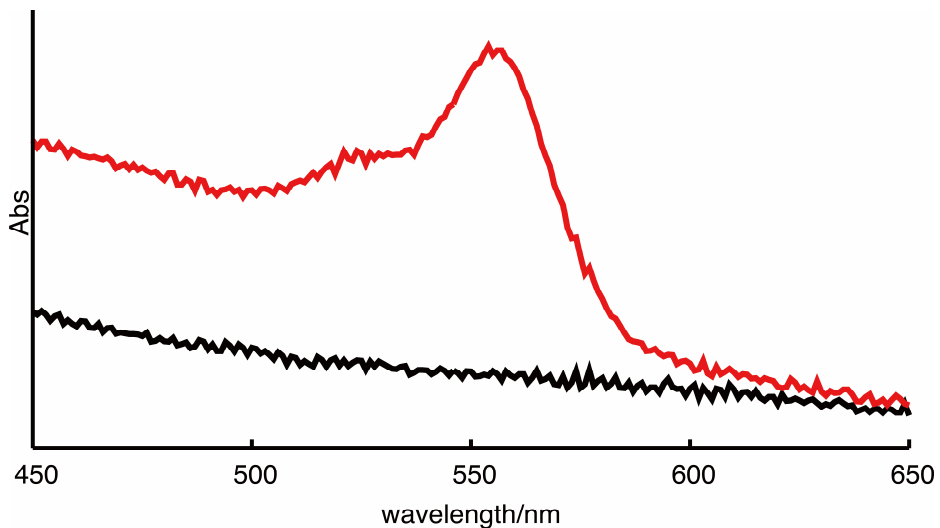


Figure S17. Absorption spectra of a PMMA film containing compound **2a** before (black line) and after (red line) UV irradiation.

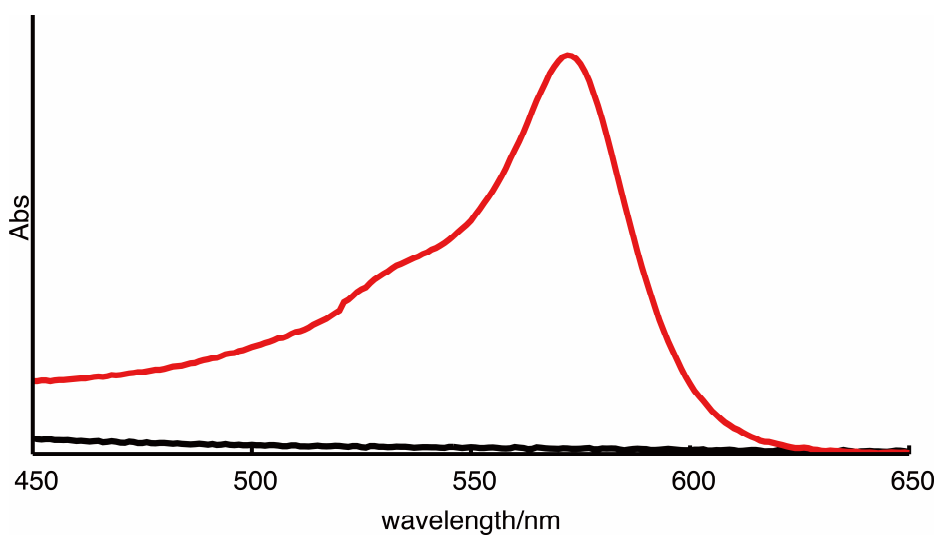


Figure S18. Absorption spectra of a PMMA film containing compound **2b** before (black line) and after (red line) UV irradiation.

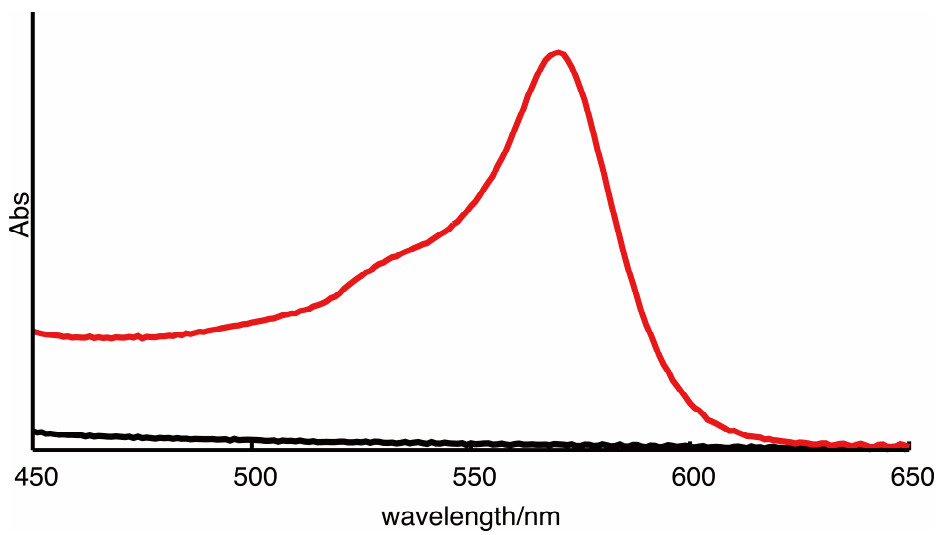


Figure S19. Absorption spectra of a PMMA film containing compound **2c** before (black line) and after (red line) UV irradiation.

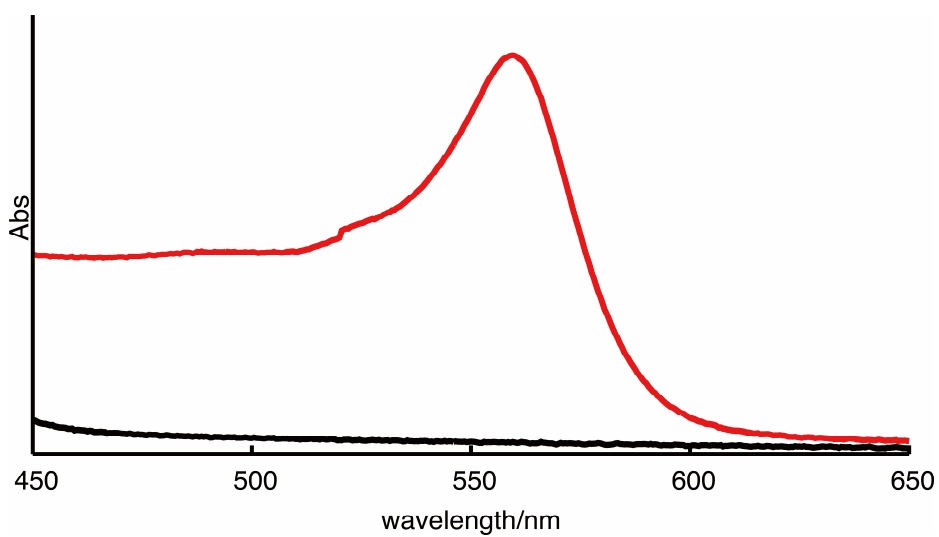


Figure S20. Absorption spectra of a PMMA film containing compound **2d** before (black line) and after (red line) UV irradiation.

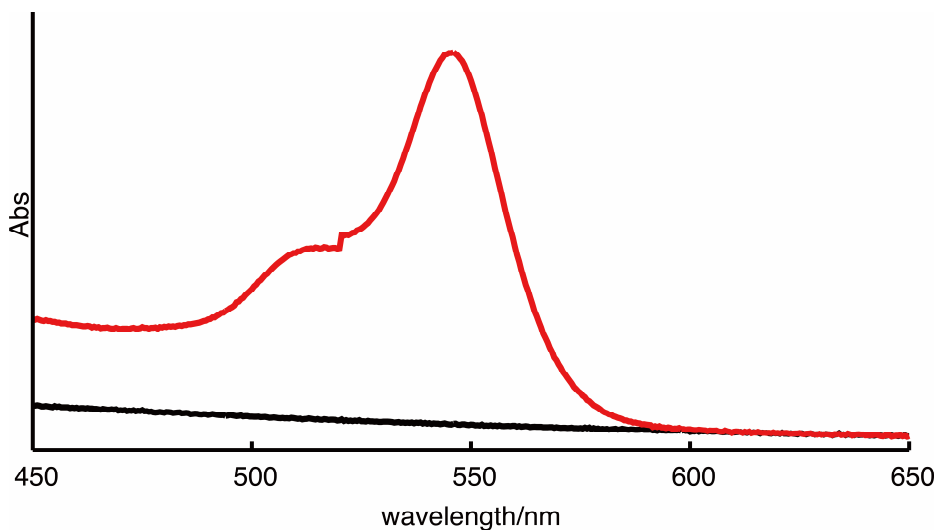


Figure S21. Absorption spectra of a PMMA film containing compound **2e** before (black line) and after (red line) UV irradiation.

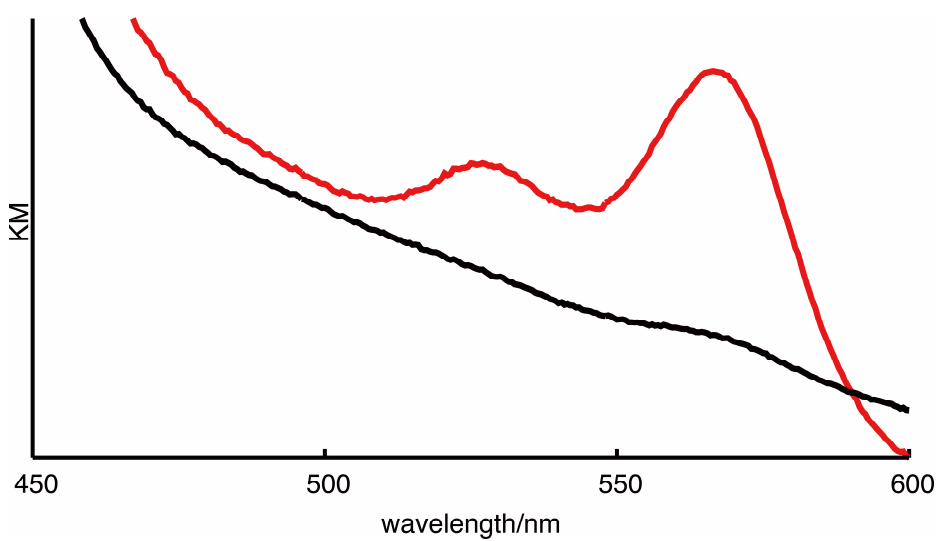


Figure S22. Diffuse reflection spectra of compound **3a** in the solid state before (black line) and after (red line) UV irradiation.

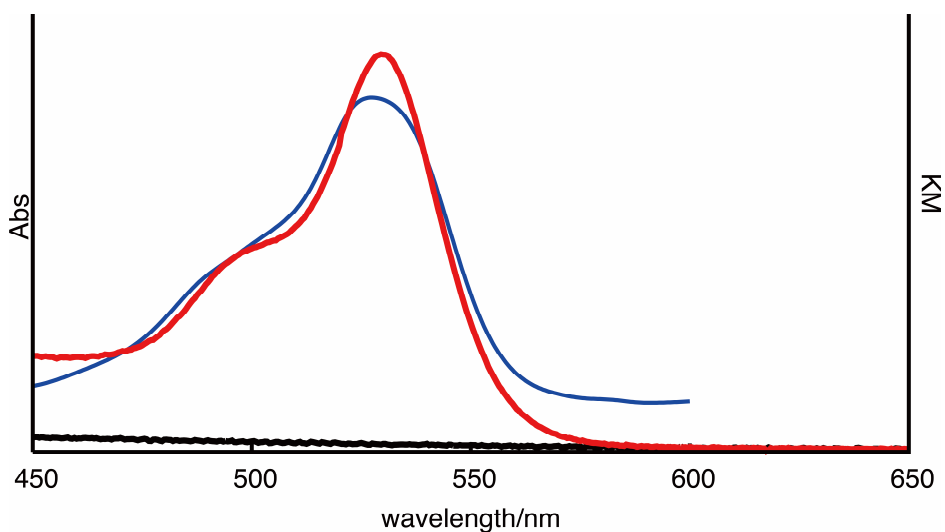


Figure S23. Absorption spectra of a PMMA film containing compound **1** before (black line) and after (red line) UV irradiation. The blue line denotes the diffuse reflection spectrum of compound **1** after UV irradiation in the solid state.

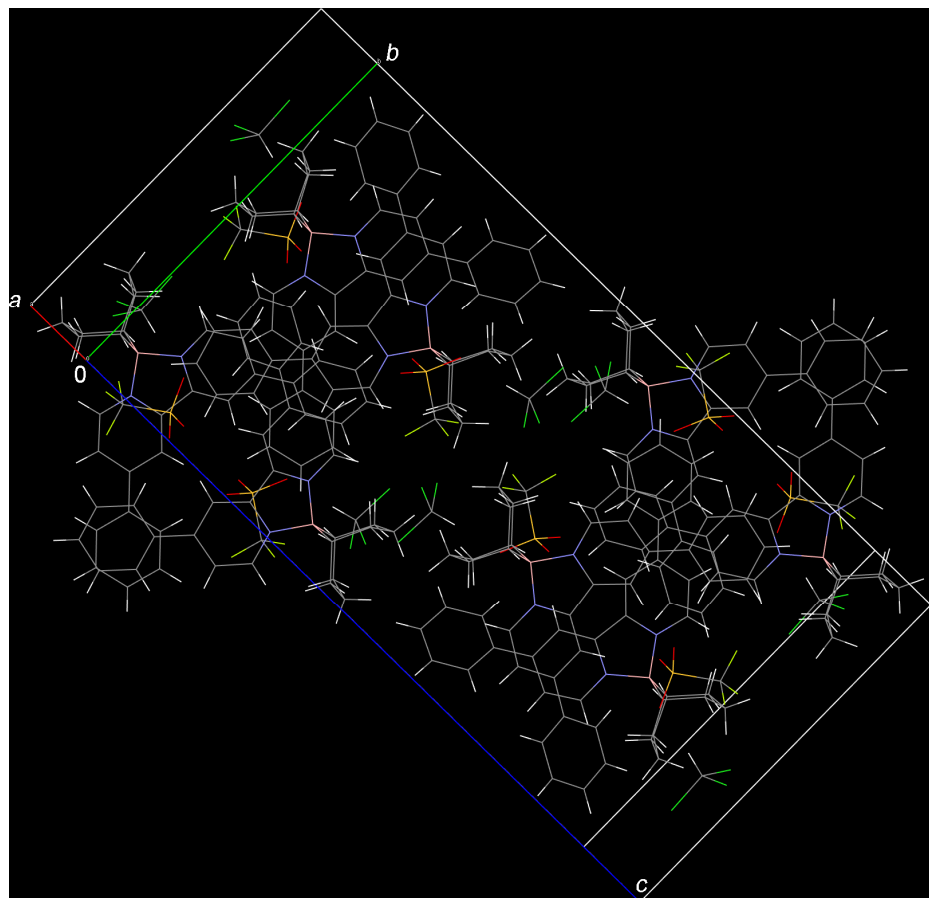


Figure S24. Packing structure of **2a**·CHCl₃ viewed along the normal direction of the (100) plane.

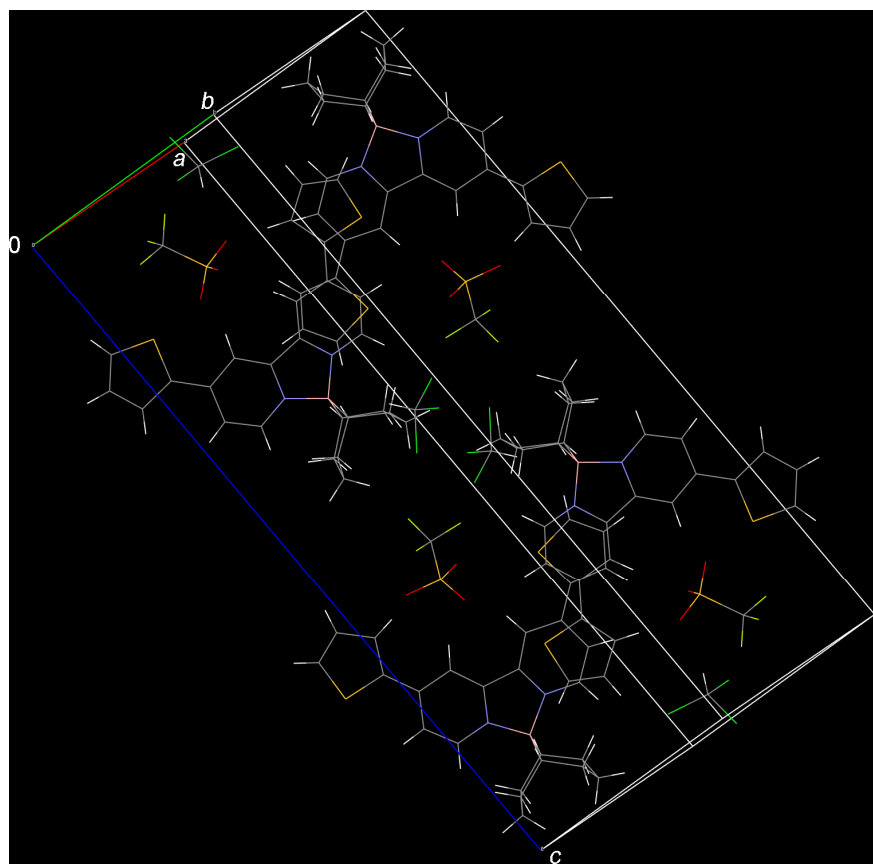


Figure S25. Packing structure of **2b**·CHCl₃ viewed along the normal direction of the (1 -1 0) plane.

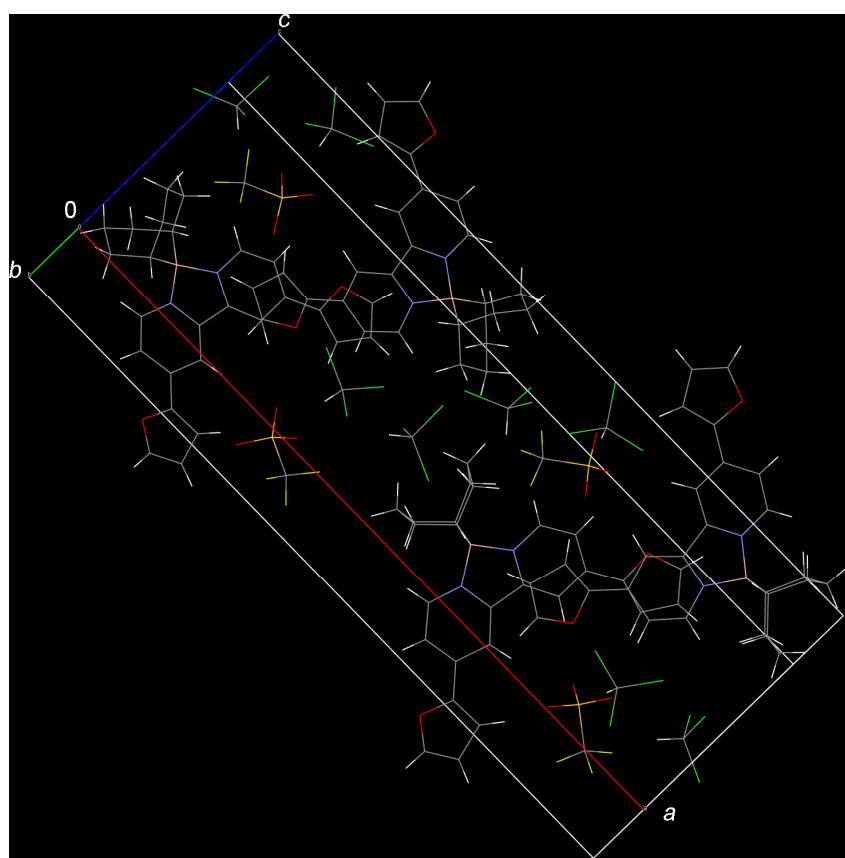


Figure S26. Packing structure of **2c**·2CHCl₃ viewed along the normal direction of the (041) plane.

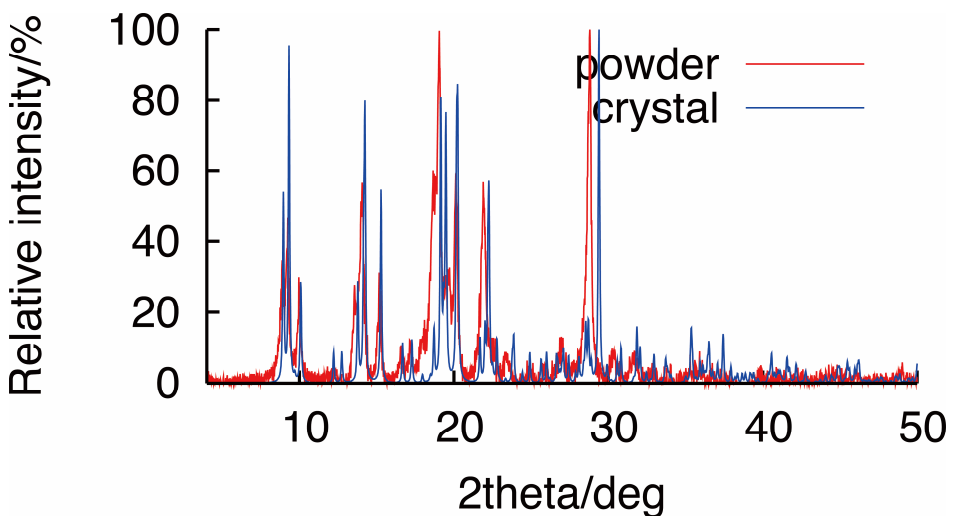


Figure S27. X-ray powder diffraction pattern of **1** (red line) and theoretical pattern estimated from the single-crystal X-ray crystallographic analysis of **1** (blue line).

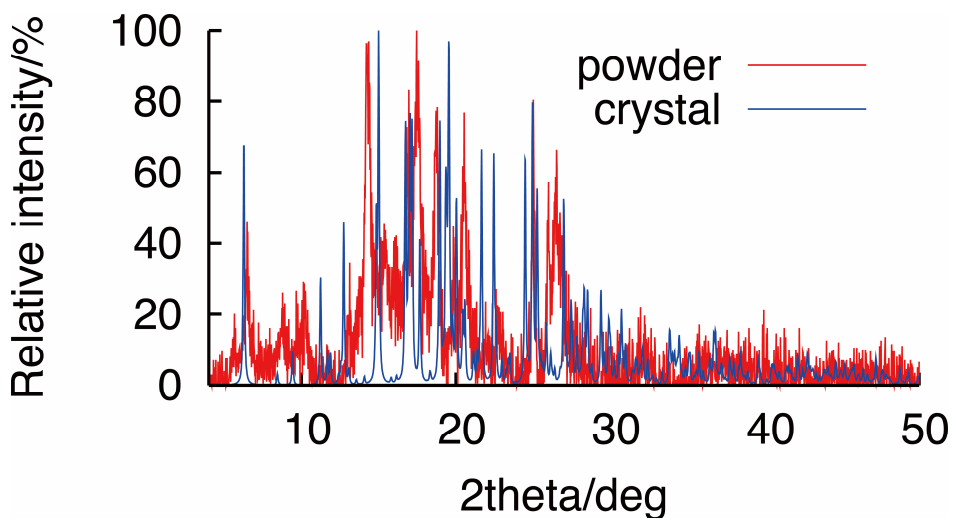


Figure S28. X-ray powder diffraction pattern of **2a** (red line) and theoretical pattern estimated from the single-crystal X-ray crystallographic analysis of **2a**·CHCl₃ (blue line).

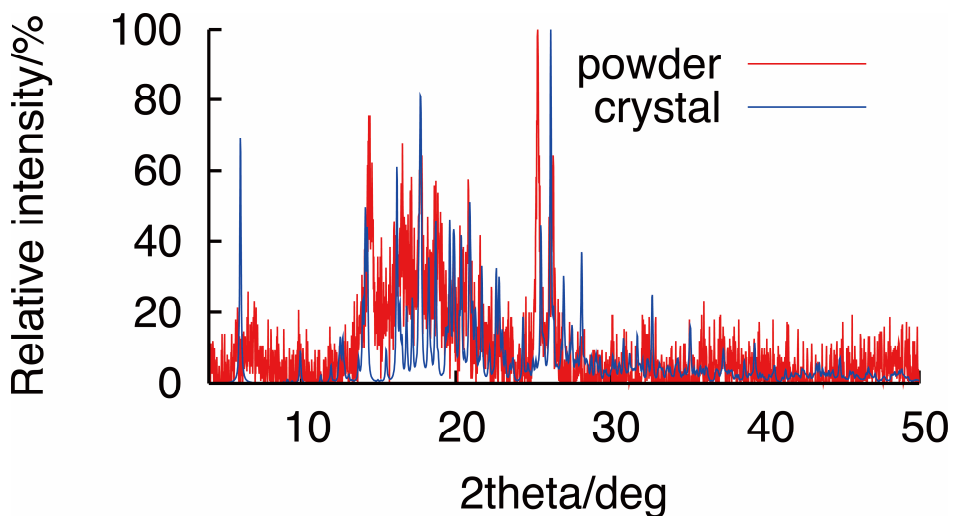


Figure S29. X-ray powder diffraction pattern of **2b** (red line) and theoretical pattern estimated from the single-crystal X-ray crystallographic analysis of **2b**·CHCl₃ (blue line).

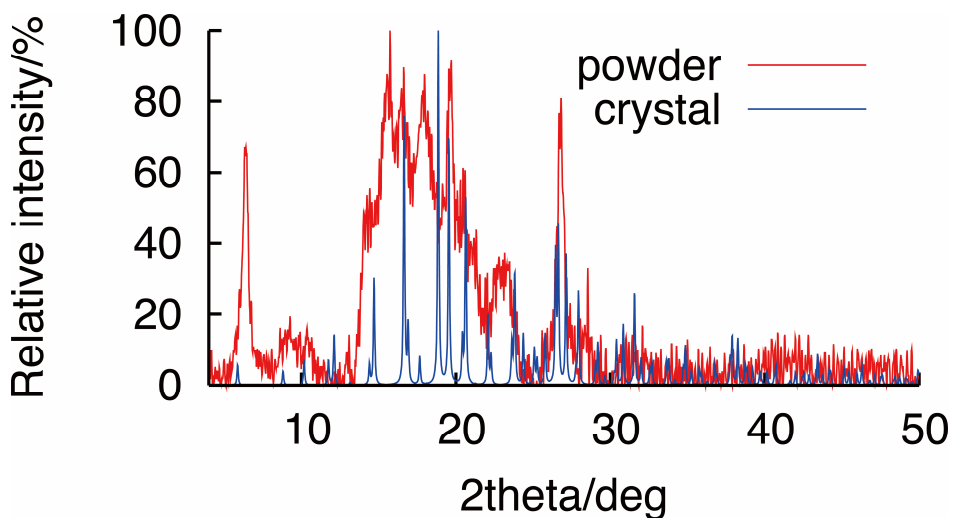
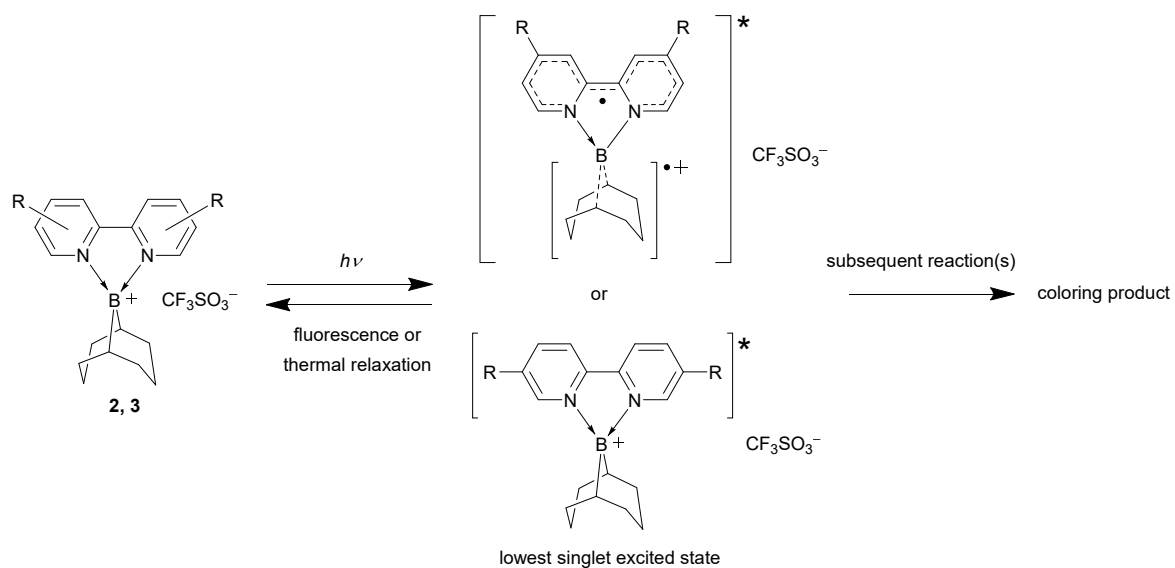
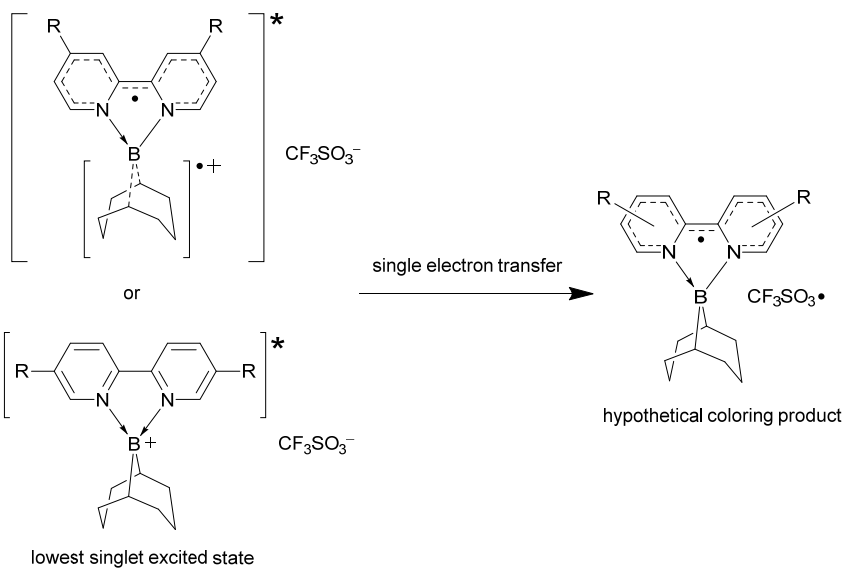


Figure S30. X-ray powder diffraction pattern of **2c** (red line) and theoretical pattern estimated from the single-crystal X-ray crystallographic analysis of **2c** · 2CHCl₃ (blue line).



Scheme S1. Two phases of the process after irradiation of the boronium complex



Scheme S2. A hypothetical reaction and coloring product in the latter half phase in Scheme S1.

2. Experimental section

General information. Solvents were purified by reported methods before use.² All reactions were carried out under an argon atmosphere unless otherwise noted. ¹H NMR (300 MHz), ¹³C NMR (76 MHz), ¹¹B NMR (96 MHz), and ¹⁹F NMR (283 MHz) spectra were measured with a JEOL JNM-ECX300 spectrometer. Tetramethylsilane was used as an internal standard for the ¹H and ¹³C NMR spectra. Boron trifluoride diethyl etherate was used as an external standard for the ¹¹B NMR spectra. Fluorobenzene was employed as an external standard for the ¹⁹F NMR spectra, using the chemical shift of -113 ppm referenced to the chemical shift of trichlorofluoromethane at 0 ppm. Low- and high-resolution mass spectra were measured with a JEOL MStation JMS-700V spectrometer. Absorption spectra of the complexes in solution and diffuse reflection spectra of the complexes in the solid state were measured with a JASCO V-570 spectrometer. Fluorescence spectra were measured with a Shimadzu RF-5300PC spectrometer. The absolute values of fluorescence quantum yields were measured by a Hamamatsu Photonics C11347 Quantaurus-QY absolute PL quantum yield spectrometer. Powder samples for diffuse reflection spectroscopy, except in the photoirradiation experiments, were diluted one thousand-fold with barium sulfate. For UV-light irradiation experiments, a UVP UVGL-25 compact UV lamp was used. For visible-light irradiation experiments, a light source and monochromator in the fluorescence spectrometer described above were used. 4,4'-Diphenyl-2,2'-bipyridine (**4a**),³ 4,4'-di(2-thienyl)-2,2'-bipyridine (**4b**),⁴ 4,4'-dimesityl-2,2'-bipyridine (**4e**),⁵ 4,4'-dibromo-2,2'-bipyridine (**4f**),³ 5,5'-diphenyl-2,2'-bipyridine (**5a**),⁶ 5,5'-di(2-thienyl)-2,2'-bipyridine (**5b**),⁷ 5,5'-di(phenylethynyl)-2,2'-bipyridine (**5d**),⁸ and 5,5'-dibromo-2,2'-bipyridine (**5f**),⁹ were prepared according to the literature. Column chromatography was performed using silica gel 60N (spherical neutral) obtained from Kanto Chemical Co., Inc. PMMA was obtained from Fujifilm Wako Pure Chemical Corporation and purified before use by dissolving in benzene (Fujifilm Wako Pure Chemical Corporation, guaranteed reagent grade), stirring overnight, dropping into methanol (Fujifilm Wako Pure Chemical Corporation, guaranteed reagent grade) with stirring, filtration, and then drying under reduced pressure (20 mmHg) at 80–150 °C for 12 h.

Synthesis of 4,4'-di(2-furyl)-2,2'-bipyridine (4c**).** Tetrahydrofuran (40 mL) containing **4f** (0.87 g, 2.8 mmol) and 2-furylboronic acid (0.70 g, 6.3 mmol, 2.3 equiv) was bubbled with nitrogen gas for 15 min before addition of aqueous sodium carbonate (2.0 M, 5.6 mL), and then bubbled again for an additional 24 min. After addition of tetrakis(triphenylphosphine)palladium(0) (0.106 g, 0.0917 mmol, 0.03 equiv), the mixture was bubbled for 16 min and then heated under reflux for 13 h in nitrogen atmosphere. After condensation of the reaction mixture under reduced pressure, it was extracted with chloroform. The organic layer was washed with water and dried over anhydrous magnesium sulfate. Evaporation of the solvents and recrystallization from chloroform afforded compound **4c** (0.608 g,

77%). **4c**: colorless powder, mp 218.0–218.5 °C. ^1H NMR (CDCl_3 , 300 MHz) δ 6.56 (dd, 2H, J = 3.4, 2.1 Hz, $\text{C}_4\text{H}_3\text{O}$), 7.03 (d, 2H, J = 3.4 Hz, $\text{C}_4\text{H}_3\text{O}$), 7.56–7.61 (m, 4H, furyl and pyridyl CH), 8.66 (dd, 2H, J = 1.7, 0.7 Hz, pyridyl CH), 8.71 (dd, 2H, J = 5.2, 0.7 Hz, CHN). $^{13}\text{C}\{\text{H}\}$ NMR (CDCl_3 , 76 MHz) δ 109.0 (CH), 112.1 (CH), 115.2 (CH), 117.8 (CH), 138.4 (quaternary C), 143.7 (CH), 149.6 (CH), 151.5 (quaternary C), 156.4 (quaternary C). HRMS (EI $^+$) m/z calcd for $\text{C}_{18}\text{H}_{12}\text{N}_2\text{O}_2$: 288.0899; found: 288.0899.

Synthesis of 4,4'-di(phenylethynyl)-2,2'-bipyridine (4d).¹⁰ A mixture of **4f** (1.5 g, 4.8 mmol), toluene (45 mL), and triethylamine (4.8 mL) was bubbled with nitrogen gas for 26 min before addition of tetrakis(triphenylphosphine)palladium(0) (0.057 g, 0.049 mmol, 0.010 equiv) and copper(I) iodide (0.019 g, 0.10 mmol, 0.02 equiv), and then bubbled again with nitrogen gas for 33 min. After addition of phenylacetylene (1.05 mL, 9.56 mmol, 2.0 equiv), the mixture was heated under reflux in nitrogen atmosphere for 13 h. The hot reaction mixture was filtered and then methanol (300 mL) was added to the filtrate. The resulting solution was chilled at –18 °C for 1 h and then the formed precipitate was collected by filtration. Separation by silica-gel column chromatography using chloroform as the eluent gave compound **4d** (1.03 g, 60%). **4d**: pale yellow powder. ^1H NMR (CDCl_3 , 300 MHz) δ 7.34–7.44 (m, 8H), 7.54–7.61 (m, 4H), 8.53–8.56 (m, 2H), 8.69 (d, 2H, J = 5.2 Hz).

Synthesis of 5,5'-di(2-furyl)-2,2'-bipyridine (5c). A mixture of **5f** (1.20 g, 3.82 mmol), 2-furylboronic acid (0.960 g, 8.58 mmol, 2.2 equiv), toluene (80 mL), ethanol (30 mL), and aqueous sodium carbonate (2 M, 30 mL) was bubbled with nitrogen gas for 20 min before addition of tetrakis(triphenylphosphine)palladium(0) (0.610 g, 0.528 mmol, 0.14 equiv). The mixture was stirred at 70 °C for 20 h. After cooling to room temperature, the reaction mixture was poured into water (100 mL) and then the organic layer was separated. The aqueous layers were extracted with ethyl acetate. The combined organic layers were washed with brine and dried over anhydrous magnesium sulfate. Evaporation of the solvents and washing with ethyl acetate afforded compound **5c** (0.824 g, 74%). **5c**: yellow solid, mp 152.0–152.8 °C. ^1H NMR (CDCl_3 , 300 MHz) δ 6.54 (dd, 2H, J = 3.4, 1.7 Hz, $\text{C}_4\text{H}_3\text{O}$), 6.82 (d, 2H, J = 3.4 Hz, $\text{C}_4\text{H}_3\text{O}$), 7.56 (d, 2H, J = 1.7 Hz, $\text{C}_4\text{H}_3\text{O}$), 8.06 (dd, 2H, J = 8.3, 2.4 Hz, pyridyl CH), 8.44 (dd, 2H, J = 8.3, 0.7 Hz, pyridyl CH), 9.00 (dd, 2H, J = 2.4, 0.7 Hz, CHN). $^{13}\text{C}\{\text{H}\}$ NMR (CDCl_3 , 76 MHz) δ 106.4, 111.6, 120.4, 126.2, 128.0, 131.1, 131.6, 142.7, 144.4. MS (EI) m/z calcd for $\text{C}_{18}\text{H}_{12}\text{N}_2\text{O}_2$: 288.0899; found: 288.0870.

Synthesis of (4,4'-diphenyl-2,2'-bipyridine-*N,N'*)(1,5-cyclooctanediyl)boronium(III) trifluoromethanesulfonate (2a). To a solution of 4,4'-diphenyl-2,2'-bipyridine (**4a**) (0.50 g, 1.6 mmol) in toluene (20 mL) was added *B*-(trifluoromethanesulfonyloxy)-9-borabicyclo[3.3.1]nonane (0.5 M hexane solution, 3.3 mL, 1.6 mmol, 1.0 equiv). The mixture was stirred at room temperature for 28 h.

The precipitate was collected by filtration and then recrystallized from acetone to give compound **2a** (0.330 g, 35%). **2a**: yellow solid, mp 278.0–280.9 °C (dec). ¹H NMR (DMSO-*d*₆, 300 MHz) δ 0.83 (s, 2H, CHB), 1.76–2.40 (m, 12H, CH₂), 7.70–7.79 (m, 6H, C₆H₅), 8.16–8.24 (m, 4H, C₆H₅), 8.42 (d, 2H, *J* = 6.2 Hz, pyridyl CH), 9.40 (d, 2H, *J* = 6.2 Hz, CHN), 9.63 (s, 2H, pyridyl CH). ¹³C{¹H} NMR (DMSO-*d*₆, 76 MHz) δ 21.9 (CH₂), 22.3 (CHB), 29.3 (CH₂), 119.9 (pyridyl CH), 120.7 (q, *J* = 322 Hz, CF₃), 124.1 (pyridyl CH), 127.9 (phenyl CH), 129.7 (phenyl CH), 131.8 (phenyl CH), 134.1 (quaternary phenyl C), 145.0 (CHN), 146.5 (quaternary pyridyl C), 153.2 (quaternary CN). ¹¹B NMR (DMSO-*d*₆, 96 MHz) δ 10.9 (line width *h*_{1/2} = 1495 Hz). ¹⁹F NMR (DMSO-*d*₆, 283 MHz) δ -76.2 (s). HRMS (FAB⁺) *m/z* calcd for C₃₀H₃₀BN₂ (cationic part): 429.2502; found: 429.2531.

Synthesis of [4,4'-di(2-thienyl)-2,2'-bipyridine-*N,N'*](1,5-cyclooctanediyi)boronium(III) trifluoromethanesulfonate (2b). A method similar to that used for the synthesis of **2a** with **4b** (0.356 g, 1.12 mmol) gave compound **2b** (0.173 g, 26%). **2b**: yellow solid, mp > 300 °C. ¹H NMR (DMSO-*d*₆, 300 MHz) δ 0.78 (s, 2H, CHB), 1.73–2.32 (m, 12H, CH₂), 7.45 (t, 2H, *J* = 4.5 Hz, C₄H₃S), 8.12 (d, 2H, *J* = 4.5 Hz, C₄H₃S), 8.21 (dd, 2H, *J* = 6.5, 1.7 Hz, pyridyl CH), 8.29 (d, 2H, *J* = 4.5 Hz, C₄H₃S), 9.23 (d, 2H, *J* = 6.5 Hz, CHN), 9.40 (d, 2H, *J* = 1.7 Hz, pyridyl CH). ¹³C{¹H} NMR (DMSO-*d*₆, 76 MHz) δ 21.9 (CH₂), 22.4 (CHB), 29.4 (CH₂), 117.6 (pyridyl CH), 120.7 (q, *J* = 324 Hz, CF₃), 122.1 (pyridyl CH), 129.9 (thienyl CH), 131.2 (thienyl CH), 133.5 (thienyl CH), 137.5 (thienyl quaternary C), 144.9 (CHN), 146.4 (pyridyl quaternary C), 146.6 (pyridyl quaternary C). ¹¹B NMR (DMSO-*d*₆, 96 MHz) δ 10.8 (line width *h*_{1/2} = 2603 Hz). ¹⁹F NMR (DMSO-*d*₆, 283 MHz) δ -76.2 (s). HRMS (FAB⁺) *m/z* calcd for C₂₆H₂₆BN₂S₂ (cationic part): 441.1630; found: 441.1616.

Synthesis of [4,4'-di(2-furyl)-2,2'-bipyridine-*N,N'*](1,5-cyclooctanediyi)boronium(III) trifluoromethanesulfonate (2c). A method similar to that used for the synthesis of **2a** with **4c** (0.508 g, 1.78 mmol) gave compound **2c** (0.437 g, 44%). **2c**: yellow solid, mp > 300 °C. ¹H NMR (DMSO-*d*₆, 300 MHz) δ 0.79 (s, 2H, CHB), 1.77–2.32 (m, 12H, CH₂), 6.96 (dd, 2H, *J* = 3.8, 1.7 Hz, C₄H₃O), 7.85 (d, 2H, *J* = 3.8 Hz, C₄H₃O), 8.21 (dd, 2H, *J* = 6.5, 1.7 Hz, pyridyl CH), 8.24 (d, 2H, *J* = 1.7 Hz, C₄H₃O), 9.29 (d, 2H, *J* = 6.5 Hz, CHN), 9.39 (d, 2H, *J* = 1.7 Hz, pyridyl CH). ¹³C{¹H} NMR (DMSO-*d*₆, 76 MHz) δ 21.9 (CH₂), 22.4 (CHB), 29.4 (CH₂), 114.1 (CH), 115.9 (CH), 116.1 (CH), 119.7 (CH), 141.7 (quaternary C), 145.1 (CH), 146.4 (quaternary C), 148.4 (CH), 148.6 (quaternary C). A signal from the carbon atom of the trifluoromethyl group was not observed because of its low intensity. ¹¹B NMR (DMSO-*d*₆, 96 MHz) δ 10.5 (line width *h*_{1/2} = 1591 Hz). ¹⁹F NMR (DMSO-*d*₆, 283 MHz) δ -76.2 (s). HRMS (FAB⁺) *m/z* calcd for C₂₆H₂₆BN₂O₂ (cationic part): 409.2087; found: 409.2081.

Synthesis of [4,4'-di(phenylethynyl)-2,2'-bipyridine-*N,N'*](1,5-cyclooctanediyi)boronium(III) trifluoromethanesulfonate (2d). A method similar to that used for the synthesis of **2a** with **4d** (0.37 g,

1.0 mmol) gave compound **2d** (0.268 g, 41%). **2d**: yellow solid, mp 278.9–280.1 °C(dec). ¹H NMR (DMSO-*d*₆, 300 MHz) δ 0.81 (s, 2H, CHB), 1.74–2.31 (m, 12H, CH₂), 7.52–7.64 (m, 6H, C₆H₅), 7.70–7.77 (m, 4H, C₆H₅), 8.13 (d, 2H, *J* = 6.2 Hz, CHN), 9.32–9.40 (m, 4H, pyridyl CH). ¹³C{¹H} NMR (DMSO-*d*₆, 76 MHz) δ 21.8 (CH₂), 22.4 (CHB), 29.2 (CH₂), 85.6 (C≡C), 100.7 (C≡C), 120.0 (phenyl quaternary C), 120.7 (q, *J* = 323 Hz, CF₃), 125.0 (CH), 128.5 (CH), 129.2 (CH), 131.1 (CH), 132.3 (CH), 136.7 (pyridyl quaternary C), 144.9 (CHN), 145.8 (quaternary CN). ¹¹B NMR (DMSO-*d*₆, 96 MHz) δ 12.8 (line width *h*_{1/2} = 2348 Hz). ¹⁹F NMR (DMSO-*d*₆, 283 MHz) δ –76.2 (s). HRMS (FAB⁺) *m/z* calcd for C₃₄H₃₀BN₂ (cationic part): 477.2502; found: 477.2482.

Synthesis of (4,4'-dimesityl-2,2'-bipyridine-*N,N'*)(1,5-cyclooctanediyi)boronium(III) trifluoromethaesulfonate (2e). A method similar to that used for the synthesis of **2e** with **4e** (0.205 g, 0.522 mmol) gave compound **2e** (0.106 g, 31%). **2e**: colorless solid, mp 165.2–173.2 °C. ¹H NMR (CDCl₃, 300 MHz) δ 1.06 (s, 2H, CHB), 1.90–2.15 (m, 18H, CH₂ and CH₃), 2.19–2.50 (m, 12H, CH₂ and CH₃), 7.00 (s, 4H, C₆H₂Me₃), 7.78 (dd, 2H, *J* = 6.2, 1.7 Hz, pyridyl CH), 8.54 (d, 2H, *J* = 1.7 Hz, pyridyl CH), 9.29 (d, 2H, *J* = 6.2 Hz, CHN). ¹³C{¹H} NMR (CDCl₃, 76 MHz) δ 20.3 (CH₃), 20.7 (CH₃), 21.6 (CH₂), 22.2 (CHB), 29.2 (CH₂), 120.1 (q, *J* = 321 Hz, CF₃), 123.5 (CH), 128.2 (CH), 128.6 (CH), 132.4 (quaternary C), 134.4 (quaternary C), 139.1 (quaternary C), 143.9 (CHN), 145.5 (quaternary CN), 157.3 (quaternary C). ¹¹B NMR (CDCl₃, 96 MHz) δ 10.0 (line width *h*_{1/2} = 492 Hz). ¹⁹F NMR (CDCl₃, 283 MHz) δ –88.5 (s). HRMS (FAB⁺) *m/z* calcd for C₃₆H₄₂BN₂ (cationic part): 513.3441; found: 513.3443.

Synthesis of (5,5'-diphenyl-2,2'-bipyridine-*N,N'*)(1,5-cyclooctanediyi)boronium(III) trifluoromethaesulfonate (3a). A method similar to that used for the synthesis of **2a** with **5a** (0.713 g, 2.31 mmol) gave compound **3a** (0.163 g, 12%). **3a**: yellow solid, mp 277.4–278.6 °C. ¹H NMR (DMSO-*d*₆, 300 MHz) δ 0.91 (s, 2H, CHB), 1.82–2.44 (m, 12H, CH₂), 7.57–7.72 (m, 6H, C₆H₅), 7.87–7.95 (m, 4H, C₆H₅), 9.09 (d, 2H, *J* = 8.6 Hz, pyridyl CH), 9.24–9.31 (m, 4H, pyridyl CH). ¹³C{¹H} NMR (DMSO-*d*₆, 76 MHz) δ 21.7 (CH₂), 21.9 (CHB), 29.5 (CH₂), 123.4 (pyridyl CH), 127.6 (phenyl CH), 129.8 (phenyl CH), 130.2 (phenyl CH), 134.1 (quaternary C), 138.9 (quaternary C), 141.4 (pyridyl CH), 141.5 (pyridyl CH), 144.4 (quaternary pyridyl C). A signal attributed to the carbon atom of the trifluoromethyl group cannot be observed due to its low intensity. ¹¹B NMR (DMSO-*d*₆, 96 MHz) δ 13.2 (line width *h*_{1/2} = 2410 Hz). ¹⁹F NMR (DMSO-*d*₆, 283 MHz) δ –77.7 (s). HRMS (FAB⁺) *m/z* calcd for C₃₀H₃₀BN₂ (cationic part): 429.2502; found: 429.2490.

Synthesis of [5,5'-di(2-thienyl)-2,2'-bipyridine-*N,N'*](1,5-cyclooctanediyi)boronium(III) trifluoromethaesulfonate (3b). A method similar to that used for the synthesis of **2a** with **5b** (0.404 g, 1.27 mmol) gave compound **3b** (0.230 g, 31%). **3b**: yellow solid, mp 271.8–272.6 °C. ¹H NMR

(DMSO-*d*₆, 300 MHz) δ 0.89 (s, 2H, CHB), 1.80–2.38 (m, 12H, CH₂), 7.35 (t, 2H, *J* = 4.1 Hz, C₄H₃S), 7.93 (d, 2H, *J* = 4.1 Hz, C₄H₃S), 7.99 (d, 2H, *J* = 4.1 Hz, C₄H₃S), 9.04 (d, 2H, *J* = 8.6 Hz, pyridyl CH), 9.13 (d, 2H, *J* = 8.6 Hz, pyridyl CH), 9.19 (s, 2H, CHN). ¹³C{¹H} NMR (DMSO-*d*₆, 76 MHz) δ 21.7 (CH₂), 21.9 (CHB), 29.3 (CH₂), 123.4 (pyridyl CH), 128.8 (thienyl CH), 129.8 (thienyl CH), 130.5 (thienyl CH), 132.8 (quaternary C), 136.4 (quaternary C), 138.9 (pyridyl CH), 139.6 (pyridyl CH), 143.7 (quaternary pyridyl C). A signal from the carbon atom of the trifluoromethyl group was not observed because of its low intensity. ¹¹B NMR (DMSO-*d*₆, 96 MHz) δ 13.6 (line width *h*_{1/2} = 2410 Hz). ¹⁹F NMR (DMSO-*d*₆, 283 MHz) δ -77.7 (s). HRMS (FAB⁺) *m/z* calcd for C₂₆H₂₆BN₂S₂ (cationic part): 441.1630; found: 441.1643.

Synthesis of [5,5'-di(2-furyl)-2,2'-bipyridine-*N,N'*](1,5-cyclooctanediyi)boronium(III) trifluoromethanesulfonate (3c). A method similar to that used for the synthesis of **2a** with **5c** (0.716 g, 2.48 mmol) gave compound **3c** (0.196 g, 14%). **3c:** yellow solid, mp 262.6–263.2 °C. ¹H NMR (DMSO-*d*₆, 300 MHz) δ 0.87 (s, 2H, CHB), 1.81–2.38 (m, 12H, CH₂), 6.83 (dd, 2H, *J* = 3.4, 1.7 Hz, C₄H₃O), 7.58 (d, 2H, *J* = 3.4 Hz, C₄H₃O), 6.07 (d, 2H, *J* = 1.7 Hz, C₄H₃O), 9.00 (d, 2H, *J* = 8.6 Hz, pyridyl CH), 9.12 (d, 2H, *J* = 8.6 Hz, pyridyl CH), 9.28 (s, 2H, CHN). ¹³C{¹H} NMR (DMSO-*d*₆, 76 MHz) δ 21.7 (CH₂), 21.8 (CHB), 29.2 (CH₂), 112.6 (furyl CH), 113.4 (furyl CH), 123.3 (pyridyl CH), 128.7 (quaternary C), 136.9 (CH), 137.8 (CH), 143.5 (quaternary C), 146.5 (pyridyl CH), 147.5 (quaternary pyridyl C). A signal from the carbon atom of the trifluoromethyl group was not observed because of its low intensity. ¹¹B NMR (DMSO-*d*₆, 96 MHz) δ 20.1 (line width *h*_{1/2} = 432 Hz). ¹⁹F NMR (DMSO-*d*₆, 283 MHz) δ -77.7 (s). HRMS (FAB⁺) *m/z* calcd for C₂₆H₂₆BN₂O₂ (cationic part): 409.2087; found: 409.2076.

Synthesis of [5,5'-di(phenylethynyl)-2,2'-bipyridine-*N,N'*](1,5-cyclooctanediyi)boronium(III) trifluoromethanesulfonate (3d). A method similar to that used for the synthesis of **2a** with **5d** (0.410 g, 1.15 mmol) gave compound **3d** (0.340 g, 47%). **3d:** yellow solid, mp 253.2–254.2 °C. ¹H NMR (DMSO-*d*₆, 300 MHz) δ 0.86 (s, 2H, CHB), 1.80–2.34 (m, 12H, CH₂), 7.48–7.57 (m, 6H, C₆H₅), 7.70–7.77 (m, 4H, C₆H₅), 8.92 (d, 2H, *J* = 8.3 Hz, pyridyl CH), 9.18 (d, 2H, *J* = 8.3 Hz, pyridyl CH), 9.24 (s, 2H, CHN). ¹³C{¹H} NMR (DMSO-*d*₆, 76 MHz) δ 21.6 (CH₂), 21.8 (CHB), 22.3 (CH₂), 84.4 (C≡C), 97.5 (C≡C), 120.7 (quaternary C), 122.8 (quaternary C), 123.5 (CH), 129.0 (CH), 130.4 (CH), 132.1 (CH), 144.4 (quaternary CN), 145.2 (CH), 145.7 (CH). ¹¹B NMR (DMSO-*d*₆, 96 MHz) δ 12.6 (line width *h*_{1/2} = 2623 Hz). ¹⁹F NMR (DMSO-*d*₆, 283 MHz) δ -77.7 (s). HRMS (FAB⁺) *m/z* calcd for C₃₄H₃₀BN₂⁺ (cationic part): 477.2502; found: 477.2482.

Preparation of PMMA films containing compound 1 and 2a–d. A solution of a boronium complex (1.0 μmol) and PMMA (0.20 g) in MeCN (2.0 mL) was stirred for 12 h and then filtered. The filtrate

(200 μ L) was dropped onto a cover glass with a side length of 18 mm, dried under natural conditions for 1 day and then heated at 80–150 °C for 12 h under the reduced pressure (20 mmHg). Films for observations were obtained by peeling off the cover glass.

Estimation of color-quenching rate constants of PMMA films. A PMMA film with a dispersed boronium complex was irradiated by UV light (365 nm) for 10 min in air and set in the optical path of the UV-vis spectrometer. Absorbance was measured every 5 min. Rate constants were estimated as slopes of the fitting lines of the natural logarithm of observed absorbance versus time.

X-ray crystallographic analysis. X-ray diffraction data for single crystals of **2a**·CHCl₃, **2b**·CHCl₃, **2c**·2CHCl₃, **3a**, and **3d** were collected using a Rigaku R-AXIS RAPID diffractometer. The structures were solved by the direct method using SHELXS Version 2013/1 and SIR92, and refined by full-matrix least-squares using SHELXL Version 2016/4, 2017/1, and 2018/1.^{11,12}

Crystal data for **2a**·CHCl₃: C₃₂H₃₁BCl₃F₃N₂O₃S, $M = 697.83$, monoclinic, $a = 14.5487(3)$ Å, $b = 15.4322(3)$ Å, $c = 28.7510(6)$ Å, $\beta = 101.544(7)^\circ$, $U = 6324.5(3)$ Å³, $T = 173$ K, space group $C2/c$ (no. 15), $Z = 8$, 30627 reflections measured, 7236 unique ($R_{\text{int}} = 0.0341$), which were used in all calculations. The final wR(F²) was 0.1210 (all data). CCDC 1946261.

Crystal data for **2b**·CHCl₃: C₂₈H₂₇BCl₃F₃N₂O₃S₃, $M = 709.88$, triclinic, $a = 9.76723(18)$ Å, $b = 10.8636(2)$ Å, $c = 29.3189(6)$ Å, $\alpha = 86.890(6)^\circ$, $\beta = 86.035(6)^\circ$, $\gamma = 85.589(6)^\circ$, $U = 3090.57(11)$ Å³, $T = 173$ K, space group $P\bar{1}$ (no. 2), $Z = 4$, 36574 reflections measured, 11081 unique ($R_{\text{int}} = 0.0517$), which were used in all calculations. The final wR(F²) was 0.2204 (all data). CCDC 1946263.

Crystal data for **2c**·2CHCl₃: C₂₉H₂₈BCl₆F₃N₂O₅S, $M = 797.13$, orthorhombic, $a = 30.1054(6)$ Å, $b = 10.64028(19)$ Å, $c = 10.64427(19)$ Å, $U = 3409.68(11)$ Å³, $T = 173$ K, space group $Pna2_1$ (no. 33), $Z = 4$, 38483 reflections measured, 6220 unique ($R_{\text{int}} = 0.1402$), which were used in all calculations. The final wR(F²) was 0.1548 (all data). CCDC 1946264.

Crystal data for **3a**: C₃₁H₃₀BF₃N₂O₃S, $M = 578.45$, triclinic, $a = 9.9951(2)$ Å, $b = 10.6777(3)$ Å, $c = 14.0199(3)$ Å, $\alpha = 68.127(5)^\circ$, $\beta = 85.063(6)^\circ$, $\gamma = 88.677(6)^\circ$, $U = 1383.34(8)$ Å³, $T = 173$ K, space group $P\bar{1}$ (no. 2), $Z = 2$, 13718 reflections measured, 6315 unique ($R_{\text{int}} = 0.0197$), which were used in all calculations. The final wR(F²) was 0.1561 (all data). CCDC 1946266.

Crystal data for **3d**: C₃₅H₃₀BF₃N₂O₃S, $M = 626.50$, triclinic, $a = 11.0952(4)$ Å, $b = 11.5436(4)$ Å, $c = 14.1018(4)$ Å, $\alpha = 112.209(8)^\circ$, $\beta = 108.743(8)^\circ$, $\gamma = 94.906(7)^\circ$, $U = 1538.71(18)$ Å³, $T = 173$ K,

space group $P\bar{1}$ (no. 2), $Z = 2$, 14994 reflections measured, 7025 unique ($R_{\text{int}} = 0.0441$), which were used in all calculations. The final $wR(F^2)$ was 0.1419 (all data). CCDC 1946267.

X-ray powder diffraction. X-ray powder diffraction patterns of **2a–c** were obtained using copper $K\alpha$ radiation on a Rigaku RINT-2200 diffractometer equipped with a scintillation detector. The diffraction patterns were collected in the range of $2\theta = 4^\circ\text{--}50^\circ$, at a scan rate of 1° min^{-1} . Theoretical X-ray powder diffraction patterns estimated from the single-crystal crystallographic analyses were calculated by Mercury 3.10.1.¹³

Theoretical calculations. All calculations were carried out at the DFT level using the B3LYP^{14, 15} exchange–correlation functional implemented in the Gaussian 09 (Revision E.01)¹⁶ suite. All calculations were performed with the 6-31G(d) basis set. The energy levels of the excited states were obtained by the time-dependent DFT method. Zero-point energy corrections were not included in the calculations. In all calculations, C_2 symmetry was imposed on the molecular structures.

Geometry (Cartesian coordinates) of **2a'**

6	0.059443	3.418715	0.276876
6	0.051882	2.965155	-1.057148
6	0.017390	0.728284	-0.137608
6	0.044813	2.526270	1.333153
6	-0.017390	-0.728284	-0.137608
6	-0.051882	-2.965155	-1.057148
6	-0.059443	-3.418715	0.276876
6	-0.044813	-2.526270	1.333153
1	0.105144	4.478341	0.498930
1	0.059335	2.874737	2.352658
1	-0.105144	-4.478341	0.498930
1	-0.059335	-2.874737	2.352658
6	-0.030134	-1.572463	-1.237692
1	0.006037	-1.151113	-2.235199
6	0.030134	1.572463	-1.237692
1	-0.006037	1.151113	-2.235199
7	-0.023969	-1.188822	1.143495
7	0.023969	1.188822	1.143495
6	-1.309632	0.026393	3.213297
1	-2.243541	0.044194	2.631498

6	1.309632	-0.026393	3.213297
1	2.243541	-0.044194	2.631498
6	1.287361	-1.310858	4.082230
1	2.110485	-1.264333	4.808350
1	1.532307	-2.172201	3.447247
6	-0.030526	-1.573863	4.853242
1	-0.018336	-0.992355	5.778515
1	-0.051808	-2.621978	5.179103
6	-1.337707	-1.257378	4.083744
1	-2.156973	-1.176819	4.811298
1	-1.618926	-2.108489	3.450141
6	-1.287361	1.310858	4.082230
1	-2.110485	1.264333	4.808350
1	-1.532307	2.172201	3.447247
6	0.030526	1.573863	4.853242
1	0.018336	0.992355	5.778515
1	0.051808	2.621978	5.179103
6	1.337707	1.257378	4.083744
1	2.156973	1.176819	4.811298
1	1.618926	2.108489	3.450141
5	0.000000	0.000000	2.241158
6	-0.063250	-3.898186	-2.198786
6	-0.706808	-3.553702	-3.401579
6	0.570118	-5.150877	-2.103685
6	-0.719894	-4.439235	-4.475653
1	-1.234680	-2.607802	-3.484788
6	0.565139	-6.029199	-3.183835
1	1.100092	-5.425404	-1.196266
6	-0.081571	-5.677351	-4.370804
1	-1.234909	-4.167041	-5.391965
1	1.070407	-6.986621	-3.100929
1	-0.089249	-6.365865	-5.210470
6	0.063250	3.898186	-2.198786
6	0.706808	3.553702	-3.401579
6	-0.570118	5.150877	-2.103685
6	0.719894	4.439235	-4.475653

1	1.234680	2.607802	-3.484788
6	-0.565139	6.029199	-3.183835
1	-1.100092	5.425404	-1.196266
6	0.081571	5.677351	-4.370804
1	1.234909	4.167041	-5.391965
1	-1.070407	6.986621	-3.100929
1	0.089249	6.365865	-5.210470

Geometry (Cartesian coordinates) of **2b'**

6	0.000043	3.418467	0.199341
6	0.000028	2.968618	-1.140036
6	0.000002	0.729431	-0.217838
6	0.000034	2.525924	1.252132
6	-0.000002	-0.729431	-0.217838
6	-0.000028	-2.968618	-1.140036
6	-0.000043	-3.418467	0.199341
6	-0.000034	-2.525924	1.252132
1	0.000071	4.477319	0.432349
1	0.000064	2.877021	2.270833
1	-0.000071	-4.477319	0.432349
1	-0.000064	-2.877021	2.270833
6	-0.000006	-1.570205	-1.316913
1	0.000012	-1.140151	-2.310495
6	0.000006	1.570205	-1.316913
1	-0.000012	1.140151	-2.310495
7	-0.000001	-1.187413	1.065289
7	0.000001	1.187413	1.065289
6	-1.309647	-0.000030	3.135743
1	-2.243812	-0.000045	2.553989
6	1.309647	0.000030	3.135743
1	2.243812	0.000045	2.553989
6	1.312703	-1.284400	4.005309
1	2.134365	-1.221736	4.731987
1	1.574975	-2.140765	3.370492
6	0.000029	-1.574109	4.775778
1	-0.000008	-0.992162	5.700876

1	0.000060	-2.622387	5.101926
6	-1.312635	-1.284491	4.005259
1	-2.134337	-1.221927	4.731901
1	-1.574796	-2.140856	3.370394
6	-1.312703	1.284400	4.005309
1	-2.134365	1.221736	4.731987
1	-1.574975	2.140765	3.370492
6	-0.000029	1.574109	4.775778
1	0.000008	0.992162	5.700876
1	-0.000060	2.622387	5.101926
6	1.312635	1.284491	4.005259
1	2.134337	1.221927	4.731901
1	1.574796	2.140856	3.370394
5	0.000000	0.000000	2.163255
6	0.000026	3.879914	-2.268530
6	0.000066	3.574551	-3.619773
16	-0.000082	5.621325	-2.047022
6	0.000105	4.713928	-4.459187
1	0.000130	2.561722	-4.006689
6	-0.000031	5.889122	-3.748980
1	0.000183	4.670332	-5.541969
1	-0.000073	6.901119	-4.132229
6	-0.000026	-3.879914	-2.268530
6	-0.000066	-3.574551	-3.619773
16	0.000082	-5.621325	-2.047022
6	-0.000105	-4.713928	-4.459187
1	-0.000130	-2.561722	-4.006689
6	0.000031	-5.889122	-3.748980
1	-0.000183	-4.670332	-5.541969
1	0.000073	-6.901119	-4.132229

Geometry (Cartesian coordinates) of **2c'**

6	-0.000054	3.424174	-0.019096
6	-0.000054	2.964296	-1.353700
6	-0.000018	0.729100	-0.444281
6	-0.000037	2.527582	1.030088

6	0.000018	-0.729100	-0.444281
6	0.000054	-2.964296	-1.353700
6	0.000054	-3.424174	-0.019096
6	0.000037	-2.527582	1.030088
1	-0.000064	4.485924	0.193295
1	-0.000026	2.874079	2.050260
1	0.000064	-4.485924	0.193295
1	0.000026	-2.874079	2.050260
6	0.000034	-1.569874	-1.543368
1	0.000030	-1.148173	-2.541452
6	-0.000034	1.569874	-1.543368
1	-0.000030	1.148173	-2.541452
7	0.000029	-1.188425	0.838966
7	-0.000029	1.188425	0.838966
6	-1.309633	-0.000054	2.909442
1	-2.243866	-0.000086	2.327749
6	1.309633	0.000054	2.909442
1	2.243866	0.000086	2.327749
6	1.312931	-1.284122	3.779378
1	2.134138	-1.220535	4.506518
1	1.576120	-2.140612	3.145222
6	0.000059	-1.574152	4.549544
1	0.000017	-0.992485	5.474830
1	0.000107	-2.622544	4.875340
6	-1.312821	-1.284252	3.779341
1	-2.134061	-1.220779	4.506454
1	-1.575886	-2.140755	3.145150
6	-1.312931	1.284122	3.779378
1	-2.134138	1.220535	4.506518
1	-1.576120	2.140612	3.145222
6	-0.000059	1.574152	4.549544
1	-0.000017	0.992485	5.474830
1	-0.000107	2.622544	4.875340
6	1.312821	1.284252	3.779341
1	2.134061	1.220779	4.506454
1	1.575886	2.140755	3.145150

5	0.000000	0.000000	1.936334
6	-0.000078	3.881306	-2.463401
6	-0.000137	3.726100	-3.832643
6	0.000047	5.031016	-4.393772
1	-0.000180	2.792420	-4.377756
6	0.000219	5.896612	-3.334997
1	0.000163	5.294936	-5.441478
1	0.000456	6.973440	-3.257159
6	0.000078	-3.881306	-2.463401
6	0.000137	-3.726100	-3.832643
6	-0.000047	-5.031016	-4.393772
1	0.000180	-2.792420	-4.377756
6	-0.000219	-5.896612	-3.334997
1	-0.000163	-5.294936	-5.441478
1	-0.000456	-6.973440	-3.257159
8	0.000201	-5.220776	-2.161973
8	-0.000201	5.220776	-2.161973

Geometry (Cartesian coordinates) of 2d'

6	0.505212	3.388266	1.164877
6	0.432451	2.933395	-0.172802
6	0.106933	0.720739	0.735985
6	0.375464	2.500092	2.213622
6	-0.106933	-0.720739	0.735985
6	-0.432451	-2.933395	-0.172802
6	-0.505212	-3.388266	1.164877
6	-0.375464	-2.500092	2.213622
1	0.662401	4.439290	1.375580
1	0.428240	2.839336	3.235256
1	-0.662401	-4.439290	1.375580
1	-0.428240	-2.839336	3.235256
6	-0.227358	-1.551857	-0.364540
1	-0.164317	-1.147748	-1.367601
6	0.227358	1.551857	-0.364540
1	0.164317	1.147748	-1.367601
7	-0.176799	-1.175637	2.018782

7	0.176799	1.175637	2.018782
6	-1.294778	0.195146	4.087105
1	-2.218586	0.334162	3.505521
6	1.294778	-0.195146	4.087105
1	2.218586	-0.334162	3.505521
6	1.107217	-1.465459	4.957124
1	1.928448	-1.523999	5.684608
1	1.240856	-2.351361	4.322962
6	-0.234459	-1.558248	5.726201
1	-0.148719	-0.987099	6.654397
1	-0.390873	-2.596085	6.048467
6	-1.489862	-1.073980	4.957804
1	-2.290842	-0.887086	5.686285
1	-1.880251	-1.881199	4.324662
6	-1.107217	1.465459	4.957124
1	-1.928448	1.523999	5.684608
1	-1.240856	2.351361	4.322962
6	0.234459	1.558248	5.726201
1	0.148719	0.987099	6.654397
1	0.390873	2.596085	6.048467
6	1.489862	1.073980	4.957804
1	2.290842	0.887086	5.686285
1	1.880251	1.881199	4.324662
5	0.000000	0.000000	3.112877
6	0.557599	3.818620	-1.261017
6	-0.557599	-3.818620	-1.261017
6	0.664447	4.593163	-2.196714
6	-0.664447	-4.593163	-2.196714
6	0.788459	5.497664	-3.282375
6	0.996676	6.872308	-3.040098
6	0.703830	5.030130	-4.611150
6	1.116857	7.754743	-4.107683
1	1.061224	7.229735	-2.017356
6	0.825381	5.922486	-5.670152
1	0.543573	3.972519	-4.795075
6	1.031619	7.282919	-5.421174

1	1.277017	8.811742	-3.918130
1	0.759808	5.559977	-6.691540
1	1.126010	7.976252	-6.251791
6	-0.788459	-5.497664	-3.282375
6	-0.996676	-6.872308	-3.040098
6	-0.703830	-5.030130	-4.611150
6	-1.116857	-7.754743	-4.107683
1	-1.061224	-7.229735	-2.017356
6	-0.825381	-5.922486	-5.670152
1	-0.543573	-3.972519	-4.795075
6	-1.031619	-7.282919	-5.421174
1	-1.277017	-8.811742	-3.918130
1	-0.759808	-5.559977	-6.691540
1	-1.126010	-7.976252	-6.251791

Geometry (Cartesian coordinates) of **2e'**

6	0.092439	3.418889	0.853917
6	0.083476	2.963195	-0.476501
6	0.023821	0.727539	0.440540
6	0.070383	2.526200	1.913029
6	-0.023821	-0.727539	0.440540
6	-0.083476	-2.963195	-0.476501
6	-0.092439	-3.418889	0.853917
6	-0.070383	-2.526200	1.913029
1	0.134053	4.480921	1.067724
1	0.086695	2.872587	2.933278
1	-0.134053	-4.480921	1.067724
1	-0.086695	-2.872587	2.933278
6	-0.049197	-1.574251	-0.660145
1	-0.029116	-1.160603	-1.661950
6	0.049197	1.574251	-0.660145
1	0.029116	1.160603	-1.661950
7	-0.035100	-1.190065	1.720544
7	0.035100	1.190065	1.720544
6	-1.309346	0.038492	3.789969
1	-2.243296	0.064321	3.208469

6	1.309346	-0.038492	3.789969
1	2.243296	-0.064321	3.208469
6	1.275626	-1.323041	4.658405
1	2.099450	-1.284240	5.384135
1	1.512192	-2.186463	4.023128
6	-0.044337	-1.573595	5.429975
1	-0.026055	-0.992598	6.355470
1	-0.075509	-2.621563	5.755460
6	-1.349133	-1.244398	4.661589
1	-2.166638	-1.154817	5.390052
1	-1.639782	-2.093169	4.029196
6	-1.275626	1.323041	4.658405
1	-2.099450	1.284239	5.384135
1	-1.512192	2.186463	4.023128
6	0.044337	1.573595	5.429975
1	0.026055	0.992598	6.355470
1	0.075509	2.621563	5.755460
6	1.349133	1.244398	4.661589
1	2.166638	1.154817	5.390052
1	1.639782	2.093169	4.029196
5	0.000000	0.000000	2.818377
6	-0.109578	-3.903248	-1.630777
6	-1.245024	-3.952945	-2.469771
6	1.000372	-4.744940	-1.874962
6	-1.247720	-4.853566	-3.538554
6	0.951977	-5.613928	-2.966799
6	-0.160213	-5.687442	-3.811827
1	-2.129542	-4.907710	-4.172704
1	1.809723	-6.253439	-3.162560
6	0.109578	3.903248	-1.630777
6	1.245024	3.952945	-2.469771
6	-1.000372	4.744940	-1.874962
6	1.247720	4.853566	-3.538554
6	-0.951977	5.613928	-2.966799
6	0.160213	5.687442	-3.811827
1	2.129542	4.907710	-4.172704

1	-1.809723	6.253439	-3.162560
6	2.469394	3.094956	-2.225482
1	2.784760	3.112548	-1.176141
1	2.302309	2.044210	-2.495278
1	3.309785	3.448753	-2.828599
6	-2.243265	4.712574	-1.010066
1	-2.602789	3.691214	-0.839903
1	-2.075021	5.163281	-0.024066
1	-3.053238	5.273225	-1.484102
6	0.173928	6.626153	-4.993498
1	-0.360054	6.189078	-5.847272
1	-0.317945	7.575272	-4.756623
1	1.194789	6.843298	-5.321726
6	-2.469394	-3.094956	-2.225482
1	-2.784760	-3.112548	-1.176141
1	-2.302309	-2.044210	-2.495278
1	-3.309785	-3.448753	-2.828599
6	2.243265	-4.712574	-1.010066
1	2.602789	-3.691214	-0.839903
1	2.075021	-5.163281	-0.024066
1	3.053238	-5.273225	-1.484102
6	-0.173928	-6.626153	-4.993498
1	0.360054	-6.189078	-5.847272
1	0.317945	-7.575272	-4.756623
1	-1.194789	-6.843298	-5.321726

Geometry (Cartesian coordinates) of 3a'

6	-0.022089	3.459199	-1.188689
6	-0.014677	2.953177	-2.501941
6	-0.003089	0.723979	-1.627365
6	-0.012560	2.525788	-0.144121
6	0.003089	-0.723979	-1.627365
6	0.014677	-2.953177	-2.501941
6	0.022089	-3.459199	-1.188689
6	0.012560	-2.525788	-0.144121
1	0.012412	2.856069	0.880323

1	-0.012412	-2.856069	0.880323
6	0.001721	-1.584300	-2.722411
1	0.003487	-1.184464	-3.730160
6	-0.001721	1.584300	-2.722411
1	-0.003487	1.184464	-3.730160
7	0.008675	-1.195376	-0.350198
7	-0.008675	1.195376	-0.350198
6	-1.310272	-0.006637	1.720071
1	-2.244547	-0.012371	1.138863
6	1.310272	0.006637	1.720071
1	2.244547	0.012371	1.138863
6	1.319639	-1.278293	2.588823
1	2.141586	-1.210768	3.314533
1	1.586626	-2.132852	1.953411
6	0.008899	-1.574021	3.360584
1	0.009390	-0.993211	4.286343
1	0.013011	-2.622601	3.685505
6	-1.307411	-1.288459	2.593997
1	-2.125478	-1.221989	3.324169
1	-1.573823	-2.147253	1.964993
6	-1.319639	1.278293	2.588823
1	-2.141586	1.210768	3.314533
1	-1.586626	2.132852	1.953411
6	-0.008899	1.574021	3.360584
1	-0.009390	0.993211	4.286343
1	-0.013011	2.622601	3.685505
6	1.307411	1.288459	2.593997
1	2.125478	1.221989	3.324169
1	1.573823	2.147253	1.964993
5	0.000000	0.000000	0.748927
1	0.041172	-3.636419	-3.344202
1	-0.041172	3.636419	-3.344202
6	0.031565	-4.908609	-0.900306
6	0.743356	-5.419855	0.199398
6	-0.673006	-5.801639	-1.726689
6	0.748891	-6.787309	0.463765

1	1.326134	-4.752915	0.829298
6	-0.669111	-7.167777	-1.456481
1	-1.254158	-5.424425	-2.563731
6	0.042055	-7.664284	-0.361819
1	1.313361	-7.169190	1.309102
1	-1.227626	-7.844047	-2.096584
1	0.046235	-8.730002	-0.153693
6	-0.031565	4.908609	-0.900306
6	-0.743356	5.419855	0.199398
6	0.673006	5.801639	-1.726689
6	-0.748891	6.787309	0.463765
1	-1.326134	4.752915	0.829298
6	0.669111	7.167777	-1.456481
1	1.254158	5.424425	-2.563731
6	-0.042055	7.664284	-0.361819
1	-1.313361	7.169190	1.309102
1	1.227626	7.844047	-2.096584
1	-0.046235	8.730002	-0.153693

Geometry (Cartesian coordinates) of **3b'**

6	-0.049311	3.461566	-1.057163
6	-0.037545	2.952306	-2.373021
6	-0.008157	0.722064	-1.497618
6	-0.024784	2.523514	-0.011612
6	0.008157	-0.722064	-1.497618
6	0.037545	-2.952306	-2.373021
6	0.049311	-3.461566	-1.057163
6	0.024784	-2.523514	-0.011612
1	0.002479	2.849872	1.013500
1	-0.002479	-2.849872	1.013500
6	0.011934	-1.585872	-2.591606
1	0.005793	-1.188300	-3.600167
6	-0.011934	1.585872	-2.591606
1	-0.005793	1.188300	-3.600167
7	0.015187	-1.196494	-0.220049
7	-0.015187	1.196494	-0.220049

6	-1.310231	-0.012203	1.850220
1	-2.244582	-0.022077	1.269361
6	1.310231	0.012203	1.850220
1	2.244582	0.022077	1.269361
6	1.325414	-1.272937	2.718911
1	2.147022	-1.202234	3.444674
1	1.596393	-2.126041	2.083252
6	0.015719	-1.573823	3.490882
1	0.014162	-0.993031	4.416620
1	0.024014	-2.622210	3.817100
6	-1.302259	-1.293633	2.724930
1	-2.120176	-1.230307	3.455513
1	-1.566076	-2.153434	2.096044
6	-1.325414	1.272937	2.718911
1	-2.147022	1.202234	3.444674
1	-1.596393	2.126041	2.083252
6	-0.015719	1.573823	3.490882
1	-0.014162	0.993031	4.416620
1	-0.024014	2.622210	3.817100
6	1.302259	1.293633	2.724930
1	2.120176	1.230307	3.455513
1	1.566076	2.153434	2.096044
5	0.000000	0.000000	0.880121
1	0.062726	-3.630645	-3.219773
1	-0.062726	3.630645	-3.219773
6	0.079296	-4.886558	-0.759316
6	0.464859	-5.509235	0.413347
1	0.833297	-4.975238	1.282727
6	-0.079012	-7.375623	-0.854957
6	0.374821	-6.923760	0.357349
1	-0.247171	-8.397284	-1.168902
1	0.641094	-7.580062	1.177642
6	-0.079296	4.886558	-0.759316
6	-0.464859	5.509235	0.413347
1	-0.833297	4.975238	1.282727
6	0.079012	7.375623	-0.854957

6	-0.374821	6.923760	0.357349
1	0.247171	8.397284	-1.168902
1	-0.641094	7.580062	1.177642
16	0.404512	6.080295	-1.949351
16	-0.404512	-6.080295	-1.949351

Geometry (Cartesian coordinates) of **3c'**

6	0.000057	3.453375	-1.140365
6	0.000039	2.952323	-2.459487
6	0.000007	0.721738	-1.578768
6	0.000043	2.522272	-0.090865
6	-0.000007	-0.721738	-1.578768
6	-0.000039	-2.952323	-2.459487
6	-0.000057	-3.453375	-1.140365
6	-0.000043	-2.522272	-0.090865
1	0.000063	2.849158	0.934866
1	-0.000063	-2.849158	0.934866
6	-0.000019	-1.585815	-2.674262
1	-0.000014	-1.185877	-3.681951
6	0.000019	1.585815	-2.674262
1	0.000014	1.185877	-3.681951
7	-0.000010	-1.196306	-0.300130
7	0.000010	1.196306	-0.300130
6	-1.310194	-0.000004	1.769871
1	-2.244739	-0.000002	1.189227
6	1.310194	0.000004	1.769871
1	2.244739	0.000002	1.189227
6	1.314062	-1.283186	2.641768
1	2.133649	-1.216136	3.370179
1	1.581829	-2.139639	2.009694
6	-0.000001	-1.573734	3.410610
1	-0.000016	-0.993002	4.336407
1	0.000006	-2.622124	3.737452
6	-1.314052	-1.283212	2.641739
1	-2.133662	-1.216202	3.370128
1	-1.581772	-2.139659	2.009637

6	-1.314062	1.283186	2.641768
1	-2.133649	1.216136	3.370179
1	-1.581829	2.139639	2.009694
6	0.000001	1.573734	3.410610
1	0.000016	0.993002	4.336407
1	-0.000006	2.622124	3.737452
6	1.314052	1.283212	2.641739
1	2.133662	1.216202	3.370128
1	1.581772	2.139659	2.009637
5	0.000000	0.000000	0.799563
1	-0.000049	-3.642553	-3.295034
1	0.000049	3.642553	-3.295034
6	-0.000082	-4.871337	-0.863130
6	-0.000105	-5.623519	0.289337
1	-0.000127	-5.254339	1.305738
6	0.000048	-6.980100	-1.479146
6	-0.000006	-6.988184	-0.113621
1	0.000168	-7.757485	-2.228002
1	0.000056	-7.859221	0.525669
6	0.000082	4.871337	-0.863130
6	0.000105	5.623519	0.289337
1	0.000127	5.254339	1.305738
6	-0.000048	6.980100	-1.479146
6	0.000006	6.988184	-0.113621
1	-0.000168	7.757485	-2.228002
1	-0.000056	7.859221	0.525669
8	-0.000143	5.707075	-1.950512
8	0.000143	-5.707075	-1.950512

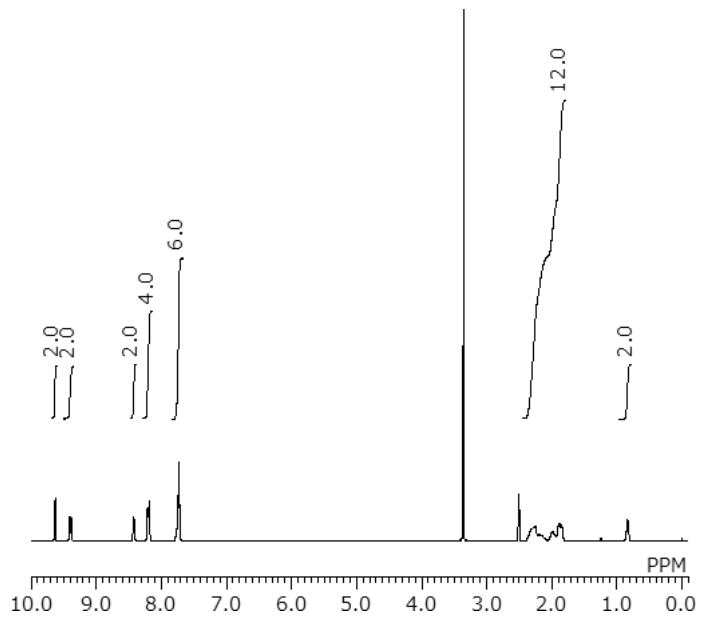
Geometry (Cartesian coordinates) of **3d'**

6	0.000005	2.949863	-2.606440
6	0.000003	0.721748	-1.719231
6	0.000003	2.521417	-0.230893
6	-0.000003	-0.721748	-1.719231
6	-0.000005	-2.949863	-2.606440
6	-0.000003	-2.521417	-0.230893

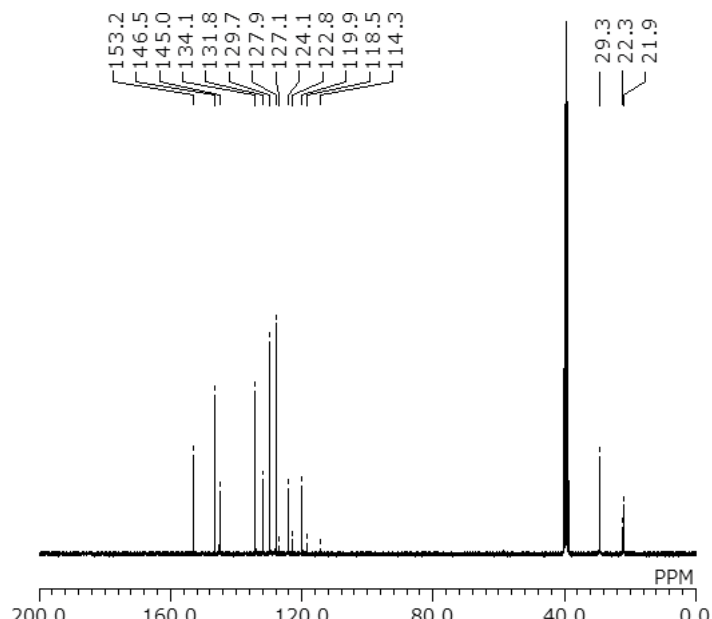
1	-0.000001	2.863448	0.790025
1	0.000001	-2.863448	0.790025
6	-0.000004	-1.582899	-2.817816
1	-0.000002	-1.179379	-3.824064
6	0.000004	1.582899	-2.817816
1	0.000002	1.179379	-3.824064
7	-0.000006	-1.195574	-0.439655
7	0.000006	1.195574	-0.439655
6	-1.310344	0.000014	1.630027
1	-2.244413	0.000020	1.048480
6	1.310344	-0.000014	1.630027
1	2.244413	-0.000020	1.048480
6	1.313553	-1.283715	2.500972
1	2.133709	-1.216815	3.228839
1	1.579751	-2.140523	1.869033
6	-0.000013	-1.573847	3.270435
1	-0.000001	-0.992803	4.196114
1	-0.000026	-2.622515	3.595319
6	-1.313579	-1.283680	2.500985
1	-2.133725	-1.216748	3.228861
1	-1.579813	-2.140486	1.869057
6	-1.313553	1.283715	2.500972
1	-2.133709	1.216815	3.228839
1	-1.579751	2.140523	1.869033
6	0.000013	1.573847	3.270435
1	0.000001	0.992803	4.196114
1	0.000026	2.622515	3.595319
6	1.313579	1.283680	2.500985
1	2.133725	1.216748	3.228861
1	1.579813	2.140486	1.869057
5	0.000000	0.000000	0.659912
1	-0.000005	-3.640528	-3.442448
1	0.000005	3.640528	-3.442448
6	0.000001	-7.422834	-0.485028
6	-0.000000	-7.877292	0.850583
6	0.000001	-8.361292	-1.538457

6	-0.000000	-9.241298	1.120437
1	-0.000001	-7.154343	1.660167
6	0.000002	-9.722773	-1.255643
1	0.000002	-8.010530	-2.565595
6	0.000001	-10.164762	0.070722
1	-0.000001	-9.587010	2.149760
1	0.000003	-10.441931	-2.069153
1	0.000001	-11.229193	0.286363
6	-0.000001	7.422834	-0.485028
6	0.000000	7.877292	0.850583
6	-0.000001	8.361292	-1.538457
6	0.000000	9.241298	1.120437
1	0.000001	7.154343	1.660167
6	-0.000002	9.722773	-1.255643
1	-0.000002	8.010530	-2.565595
6	-0.000001	10.164762	0.070722
1	0.000001	9.587010	2.149760
1	-0.000003	10.441931	-2.069153
1	-0.000001	11.229193	0.286363
6	-0.000003	-3.453323	-1.285271
6	0.000003	3.453323	-1.285271
6	-0.000001	-4.836184	-1.004896
6	0.000001	4.836184	-1.004896
6	0.000000	-6.031187	-0.765978
6	-0.000000	6.031187	-0.765978

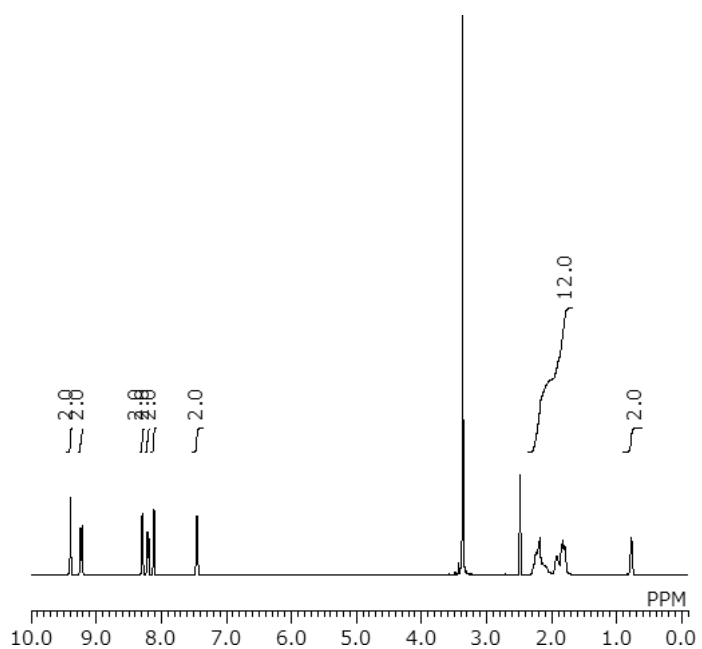
3. NMR spectra



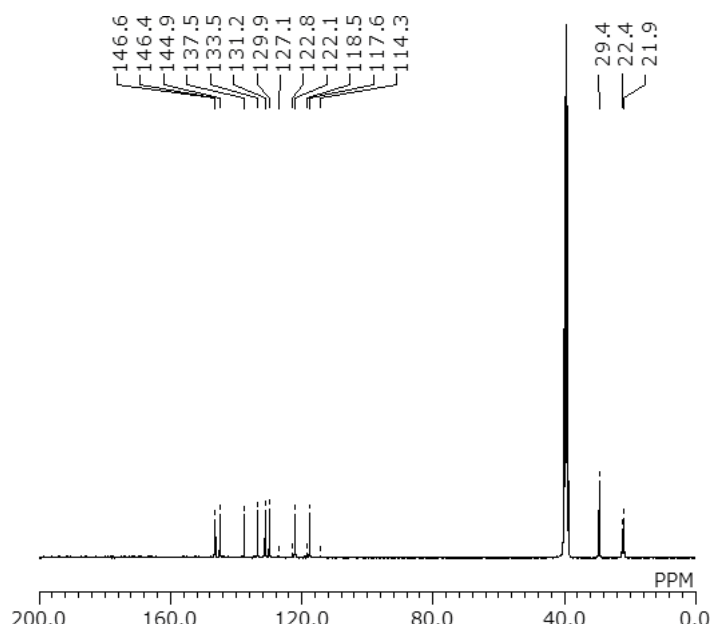
¹H NMR spectrum of compound **2a** (DMSO-*d*₆, 300 MHz).



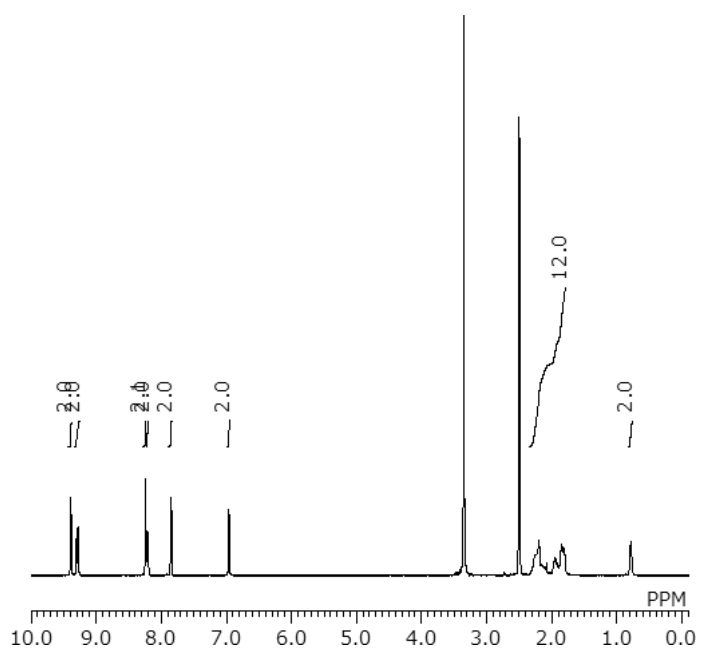
¹³C NMR spectrum of compound **2a** (DMSO-*d*₆, 76 MHz).



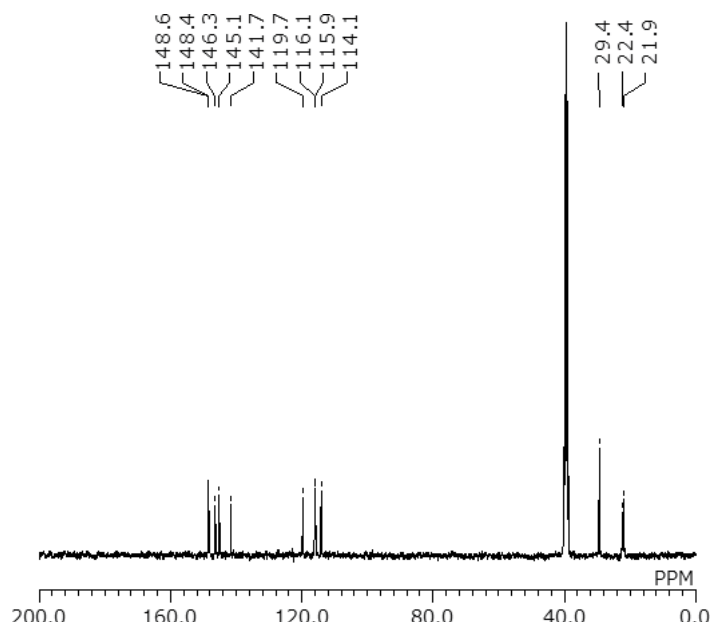
¹H NMR spectrum of compound **2b** (DMSO-*d*₆, 300 MHz).



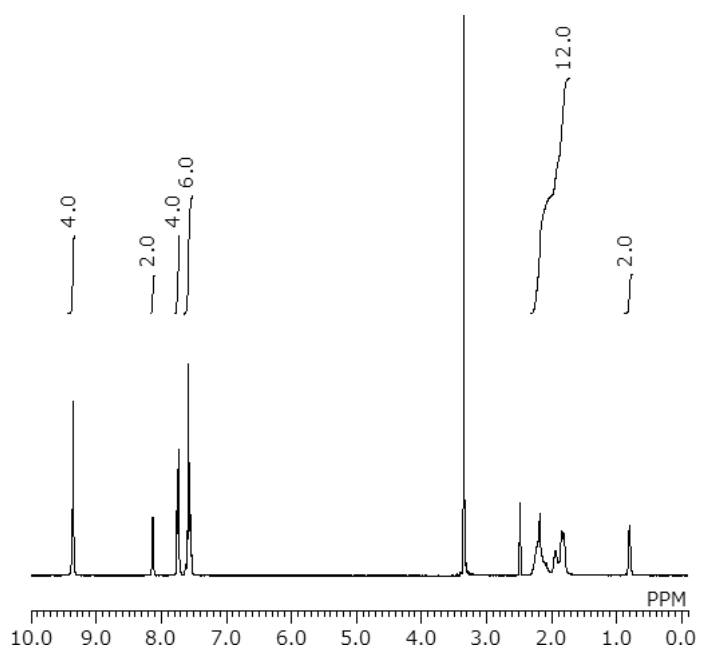
¹³C NMR spectrum of compound **2b** (DMSO-*d*₆, 76 MHz).



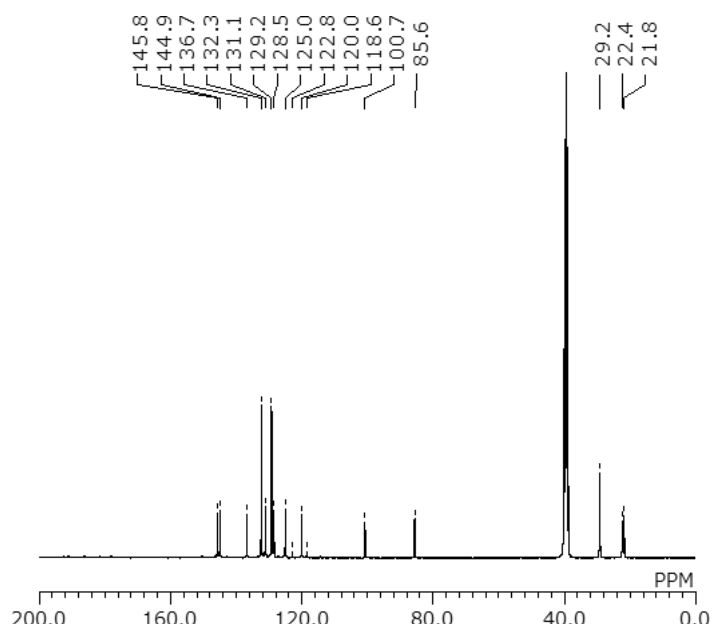
¹H NMR spectrum of compound **2c** (DMSO-*d*₆, 300 MHz).



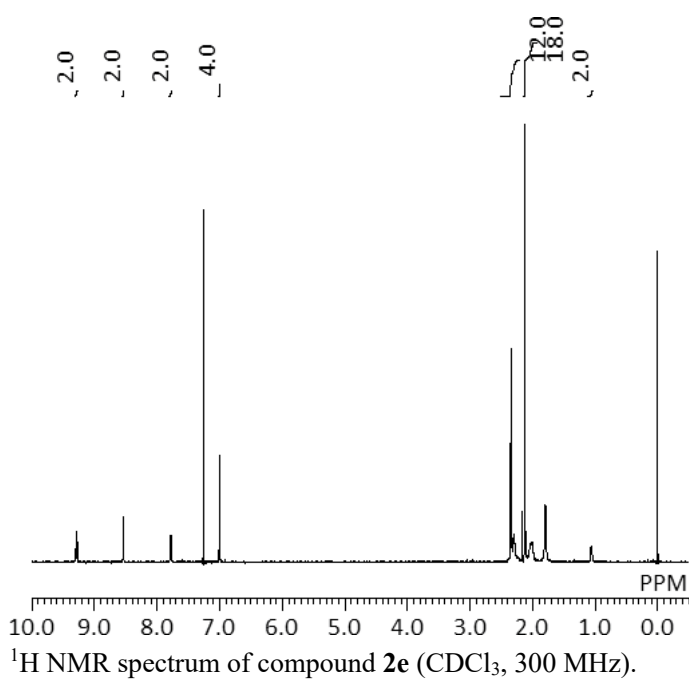
¹³C NMR spectrum of compound **2c** (DMSO-*d*₆, 76 MHz).



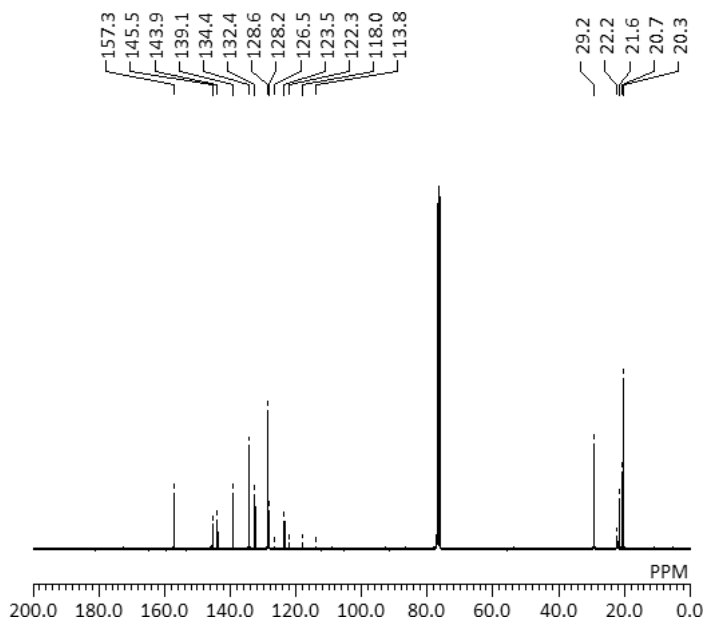
¹H NMR spectrum of compound **2d** (300 MHz, CDCl₃).



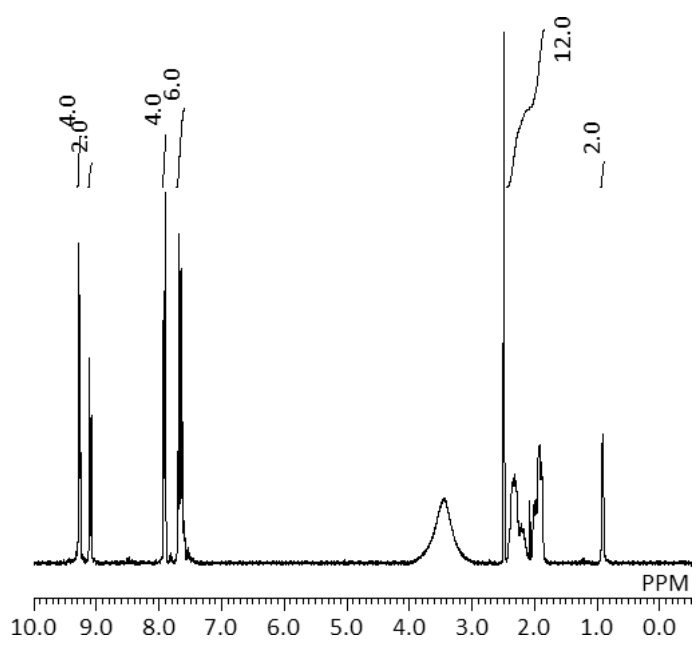
¹³C NMR spectrum of compound **2d** (76 MHz, CDCl₃).



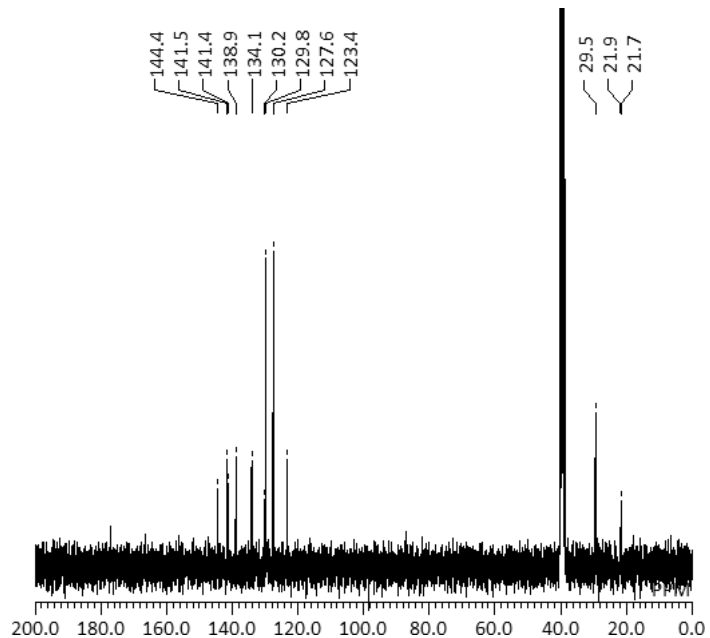
¹H NMR spectrum of compound **2e** (CDCl_3 , 300 MHz).



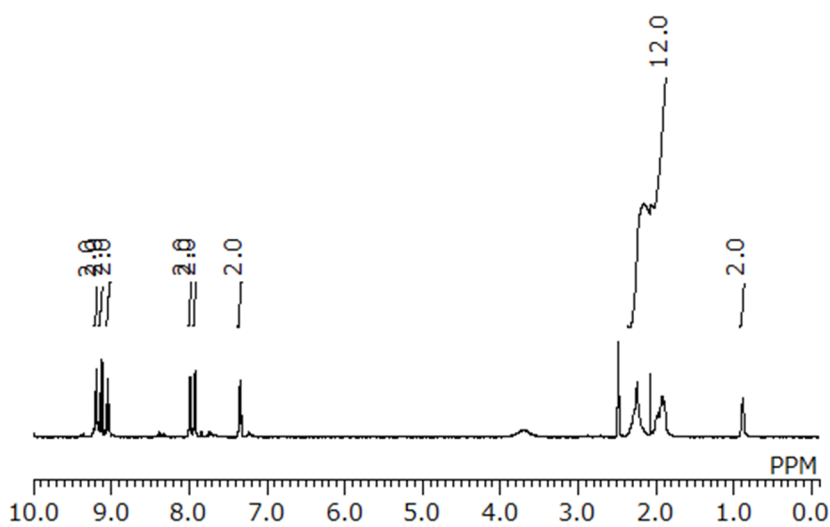
¹³C NMR spectrum of compound **2e** (CDCl_3 , 76 MHz).



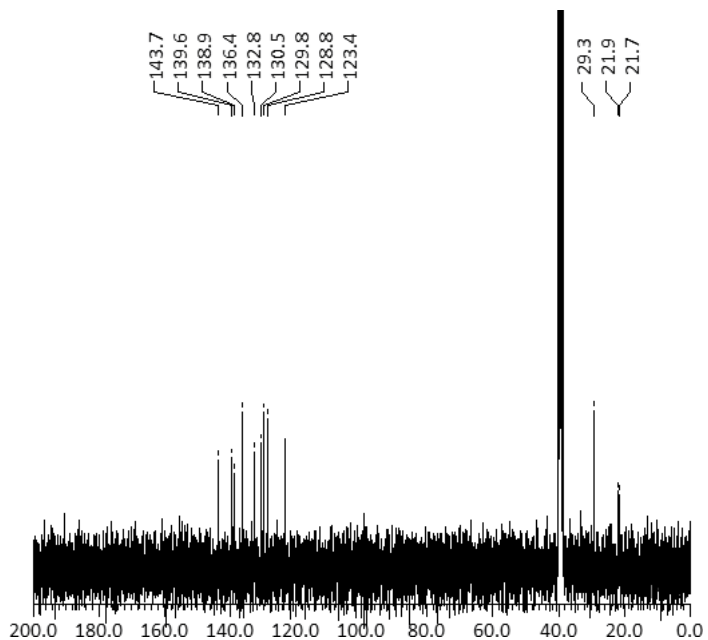
¹H NMR spectrum of compound 3a (DMSO-*d*₆, 300 MHz).



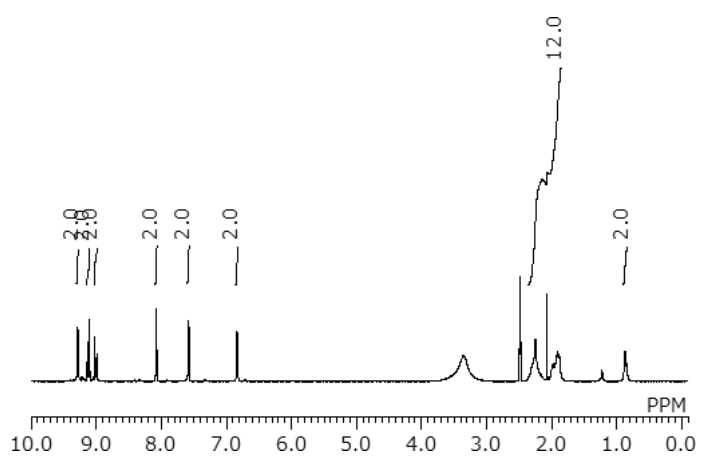
¹³C NMR spectrum of compound 3a (DMSO-*d*₆, 76 MHz).



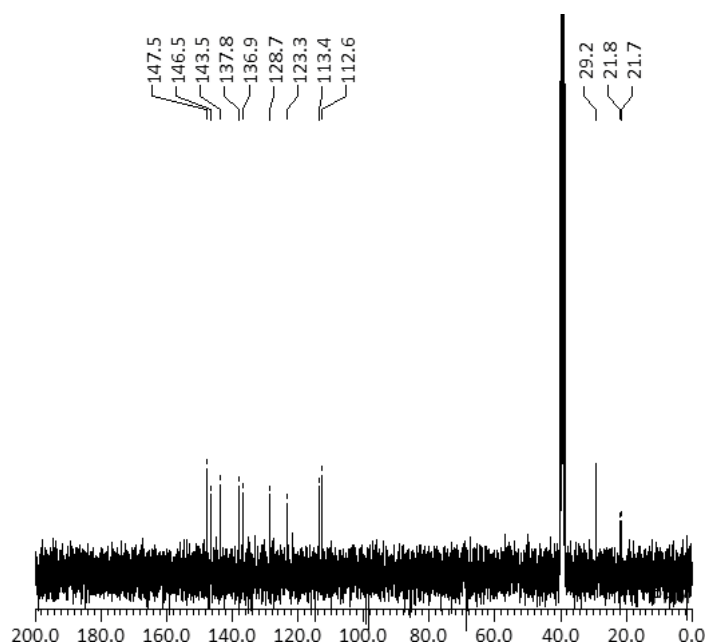
¹H NMR spectrum of compound **3b** (DMSO-*d*₆, 300 MHz).



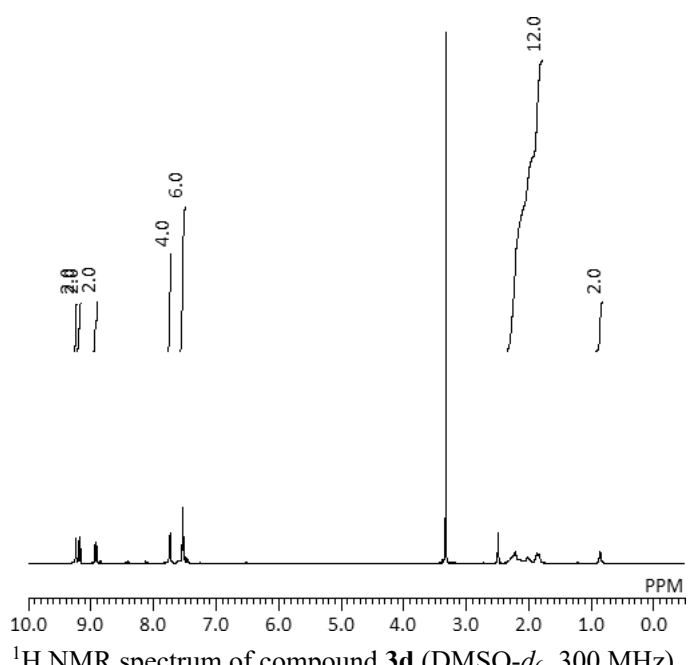
¹³C NMR spectrum of compound **3b** (DMSO-*d*₆, 76 MHz).



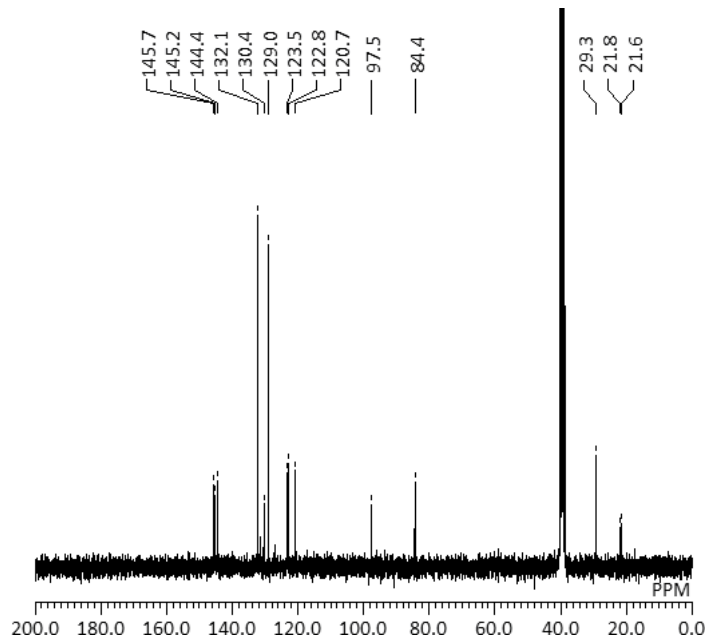
¹H NMR spectrum of compound **3c** (DMSO-*d*₆, 300 MHz).



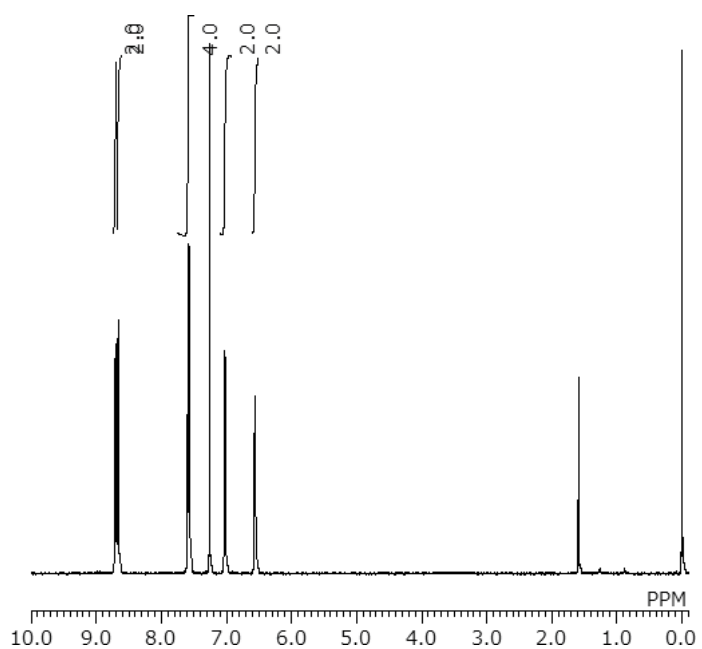
¹³C NMR spectrum of compound **3c** (DMSO-*d*₆, 76 MHz).



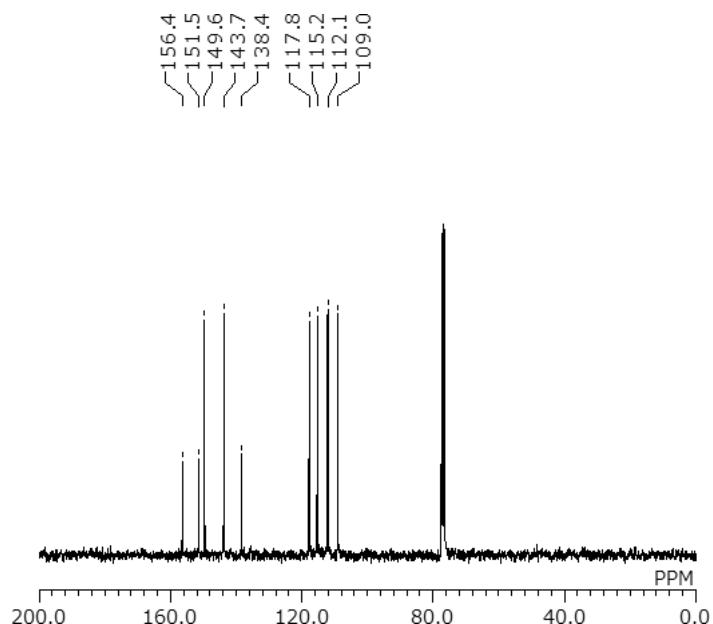
¹H NMR spectrum of compound **3d** (DMSO-*d*₆, 300 MHz).



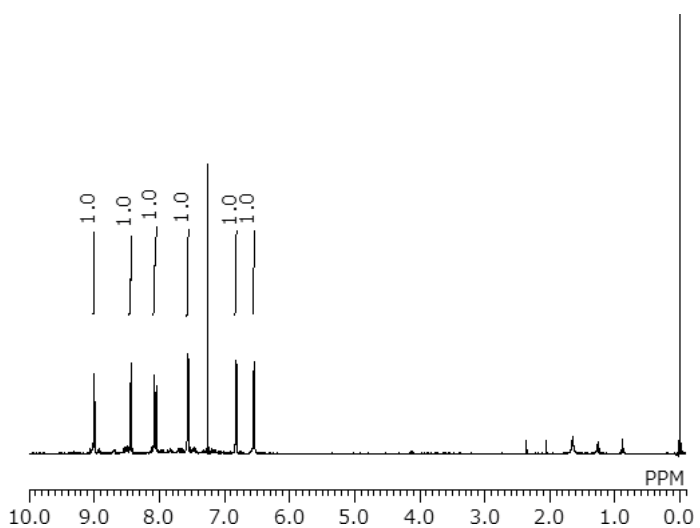
¹³C NMR spectrum of compound **3d** (DMSO-*d*₆, 76 MHz).



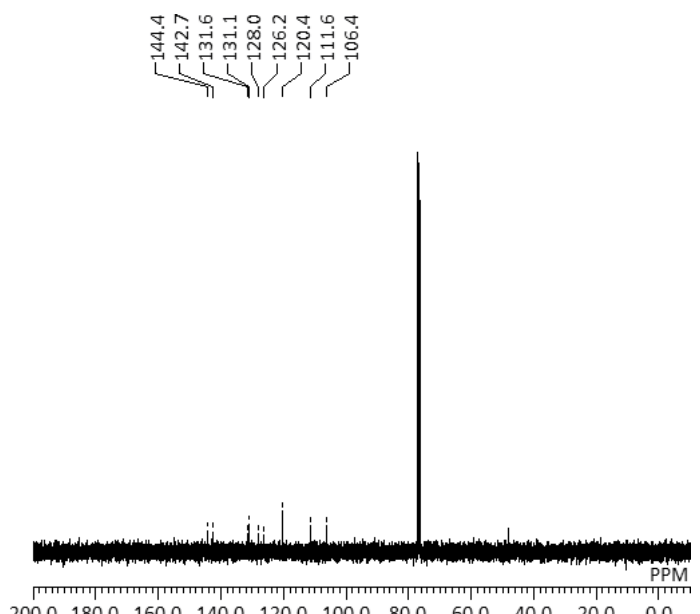
¹H NMR spectrum of compound **4c** (CDCl₃, 300 MHz).



¹³C NMR spectrum of compound **4c** (CDCl₃, 76 MHz).



¹H NMR spectrum of compound **5c** (CDCl₃, 300 MHz).



¹³C NMR spectrum of compound **5c** (CDCl₃, 76 MHz).

4. References

- 1 J. Yoshino, T. Sekikawa, N. Hatta, N. Hayashi and H. Higuchi, *Tetrahedron Lett.*, 2016, **57**, 5489.
- 2 W. L. F. Armarego and C. L. L. Chai, *Purification of Laboratory Chemicals*, 6th Edition, Butterworth-Heinemann, Elsevier, Burlington, 2009.
- 3 W.-S. Han, J.-K. Han, H.-Y. Kim, M. J. Choi, Y.-S. Kang, C. Pac and S. O. Kang, *Inorg. Chem.*, 2011, **50**, 3271.
- 4 M. B. Majewski, J. G. Smith, M. O. Wolf and B. O. Patrick, *Eur. J. Inorg. Chem.*, **2016**, 1470.
- 5 M. Chandrasekharam, G. Rajkumar, C. S. Rao, T. Suresh, M. A. Reddy, P. Y. Reddy, Y. Soujanya, B. Takeru, Y. Jun-Ho, M. K. Nazeeruddin and M. Graetzl, *Synth. Metals*, 2011, **161**, 1098.
- 6 H.-J. Nie, J.-Y. Shao, J. Wu, J. Yao and Y.-W. Zhong, *Organometallics*, 2012, **31**, 6952.
- 7 S.-J. Liu, Q. Zhao, Q.-L. Fan and W. Huang, *Eur. J. Inorg. Chem.*, 2018, **13**, 2177.
- 8 K. Oppelt, D. A. M. Egbe, U. Monkowius, M. List, M. Zabel, N. S. Sariciftci and G. Knör, *J. Organomet. Chem.*, 2011, **696**, 2252.
- 9 S. Hug, L. Stegbauer, H. Oh, M. Hirscher and B. V. Lotsch, *Chem. Mater.*, 2015, **27**, 8001.
- 10 P. V. James, K. Yoosaf, J. Kumar, K. G. Thomas, A. Listorti, G. Accorsi and N. Armaroli, *Photochem. Photobiol. Sci.*, 2009, **8**, 1432.
- 11 SHELXS Version 2013/1, SHELXL Version 2016/4, 2017/1, and 2018/1: G. M. Sheldrick, *Acta Cryst. A*, 2008, **64**, 112.
- 12 SIR92: A. Altomare, G. Cascarano, C. Giacovazzo and A. Guagliardi, *J. Appl. Cryst.*, 1993, **26**, 343.
- 13 Mercury 3.10.1: C. F. Macrae, P. R. Edgington, P. McCabe, E. Pidcock, G. P. Shields, R. Taylor, M. Towler and J. van de Streek, *J. Appl. Cryst.*, 2006, **39**, 453.
- 14 A. D. Becke, *J. Chem. Phys.*, 1993, **98**, 5648.
- 15 C. Lee, W. Yang and R. G. Parr, *Phys. Rev. B*, 1988, **37**, 785.
- 16 Gaussian 09, Revision E.01, M. J. Frisch, G. W. Trucks, H. B. Schlegel, G. E. Scuseria, M. A. Robb, J. R. Cheeseman, G. Scalmani, V. Barone, B. Mennucci, G. A. Petersson, H. Nakatsuji, M. Caricato, X. Li, H. P. Hratchian, A. F. Izmaylov, J. Bloino, G. Zheng, J. L. Sonnenberg, M. Hada, M. Ehara, K. Toyota, R. Fukuda, J. Hasegawa, M. Ishida, T. Nakajima, Y. Honda, O. Kitao, H. Nakai, T. Vreven, J. A. Montgomery, Jr., J. E. Peralta, F. Ogliaro, M. Bearpark, J. J. Heyd, E. Brothers, K. N. Kudin, V. N. Staroverov, T. Keith, R. Kobayashi, J. Normand, K. Raghavachari, A. Rendell, J. C. Burant, S. S. Iyengar, J. Tomasi, M. Cossi, N. Rega, J. M. Millam, M. Klene, J. E. Knox, J. B. Cross, V. Bakken, C. Adamo, J. Jaramillo, R. Gomperts, R. E. Stratmann, O. Yazyev, A. J. Austin, R. Cammi, C. Pomelli, J. W. Ochterski, R. L. Martin, K. Morokuma, V. G. Zakrzewski, G. A. Voth, P. Salvador, J.

J. Dannenberg, S. Dapprich, A. D. Daniels, O. Farkas, J. B. Foresman, J. V. Ortiz, J. Cioslowski and D. J. Fox, Gaussian, Inc., Wallingford CT, 2013.